

We would like to thank the anonymous referee for providing his careful and very constructive comments on our manuscript. We think to be able to address his suggestions and without doubt his contribution has resulted to significant improvement of the manuscript.

General comments:

The authors present a very interesting study on precipitation and temperature trends in the Everest region between 1994 and 2013. They analyze high altitude datasets gathered by the EV-K2-CNR project and they compare those high altitude data to other datasets which are regionally available. They draw several interesting conclusion: (i) The minimum temperature increases much stronger than the maximum temperature at high altitude, (ii) the temperature trends are stronger than for the surrounding areas; (iii) there is a significant negative trend in precipitation. This factors combined will have a very strong impact on the glaciers in the region, which is supported by recent observations of geodetic mass balances and flow velocities of the glaciers in the Khumbu region. The paper is generally well written and it is suitable for publication in the Cryosphere.

Thanks very much for the positive feedback.

The detection of precipitation trends is essential; however those measurements are conducted using tipping buckets, which are unreliable for snow fall. The authors touch upon this topic briefly (p5917), however I do not find this discussion convincing. Temperatures at the 5050 reference altitude only above zero for a limited period of time. The authors state that more than 90% of annual precipitation falls during the monsoon, but how can this be proven if only observation during the monsoon months can be trusted. It could be that there has been a shift in precipitation from the monsoon to other (colder) seasons which remains undetected because of the tipping buckets. This should be more extensively discussed.

Response:

We followed the suggestion adding some new analysis and writing a new paragraph in the data section. Moreover we provided new supporting materials (3) in order to increase the clarity on the magnitude of the possible underestimation of the solid phase of precipitation at the PYRAMID station.

“The Prec sensors at these locations are conventional heated tipping buckets which may not fully capture the solid Prec. Therefore, solid Prec is probably underestimated, especially in winter. However, in order to know the magnitude of the possible underestimation of the solid phase, we compared the monthly mean Prec of the reconstructed PYRAMID series (1994-2013 period) with the Prec of a station located downstream at 2619 m a.s.l. (Chaurikhark, ID 1202), (Fig. 1b, Table 2) which presents monthly mean temperature above 0 °C even during the winter and thus a high prevalence of liquid Prec also during these months. This comparison, supported by the elevated correlation existing between the monthly Prec of the two stations, shown a slight underestimation of the PYRAMID snow (about $3\pm 1\%$ of total annual precipitation registered at PYRAMID, see Supplementary material 3 for more details). Therefore, being much reduced the underestimation, we decided not to manipulate data.”

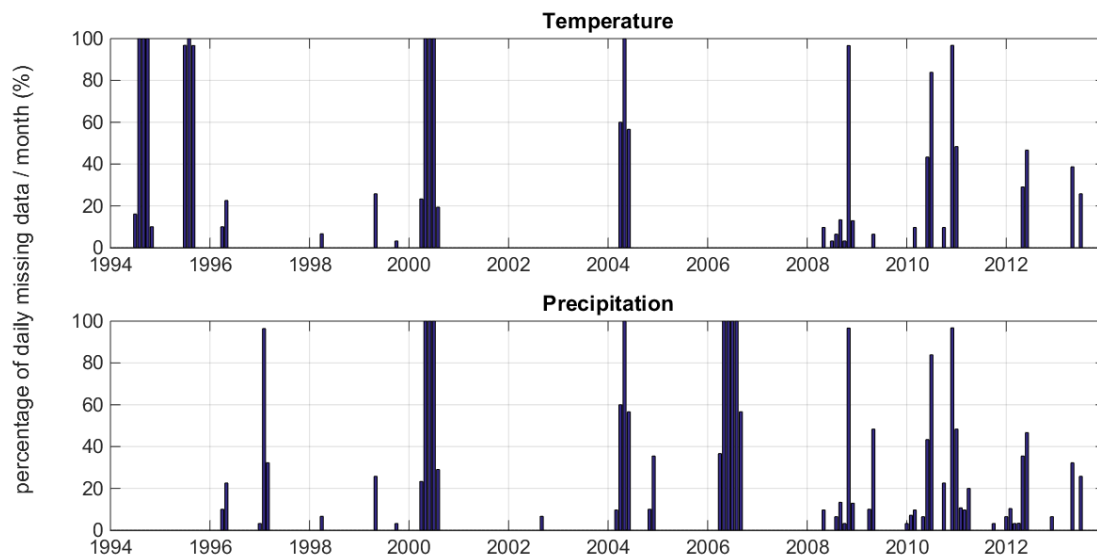
The authors reconstruct a P and T series at an altitude of 5050 and they use a quantile mapping approach to fill in missing data. It would be interesting to know how the percentage of missing data progresses with time, so it can be excluded that false trends may be attributed to trends in missing data occurrence.

Response:

We fully agree that missing data are a key issue in the assessment of the non-stationarity. To be sure about false trends possibly attributable to missing data, we dedicated several efforts to address this potential issue. In fact, the authors consider suitably the impact of missing data computing both the daily and monthly uncertainty. The applied methodology and the impact on missing data on the estimated trends is fully detailed in the supplementary materials. All uncertainty values are reported in table S3, S4 and S5. Moreover, figure S1 gives an overview of the missing data for the overall dataset used for the reconstruction.

To explicitly address the reviewer concern, the following figure reports (at monthly scale) the number of missing daily values at Pyramid both for temperature and precipitation. Concerning temperature, missing data clearly decrease after 2000, while precipitation have a maximum of missing data during the early and mid-2000s.

p.s. this new figure will be not inserted in the manuscript.



Very limited information is provided about the sensors which have been to measure the temperature and precipitation and whether they have been the same for the entire period or whether replacements have been made that may have interrupted the data series.

Response:

We followed the suggestion inserting the information related to the sensors used in the reconstruction in the Supplementary material (Table S2).

The minimum temperature trends seem extremely large (~ 0.2 degrees Celsius / year) for some months. I am not sure if this is realistic.

Response:

Yes, it is impressive! ... this increase has been experienced as unbelievable for us too (even + 4 °C over twenty years). However we completely exclude a systematic error confined to the minimum temperature and just to few months.

p.s. a curiosity: consider that our temperature trend are personally experienced by the Pyramid staff which reports that, in the recent years in November and December, outside the laboratories (5050 m) the temperature during the day, but also during the night, is often above zero (experienced as .. “a milder climate during those months in the last years”).

I really appreciate Figure 4, but I suggest for precipitation the color scheme is change. Now blue = drying , which is counterintuitive.

Response:

We appreciate the compliments, and we are working to make available the Matlab[®] script creating this figure for the community. We can understand that the color codes are counterintuitive for precipitation, but we think it is better to keep the same codes for both precipitation and temperature rather than two different color codes (if we reverse the color code for both, we will obtain blue = warming for temperature). It is also interesting to note that the color codes refer to the trend significance rather than the amplitude, having thus no units.

The P-H relation in Figure 5 is also very interesting, but it could be related a bit more to other studies in this field , the regional context and the underlying patterns that would explain this relation.

Response:

We followed the suggestion inserting this new paragraph:

“Physically, we can interpret the Prec gradient of Fig. 5a considering that when the humid air masses coming from the Bay of Bengal collide with the orographic barrier, heavy convections induce huge quantity of rain below 2500 m a.s.l.. The topographic barrier of the Himalayan mountain range causes the mechanical lift of the humid air, the cooling of the air column, the condensation and the consequent rainfall. The further increase in relief induces a depletion of the moisture content resulting in a severe reduction of Prec at higher altitudes. Our study, based on ground stations, confirms the general Prec gradient detected with the TRMM microwave observations, even if we did not identified a marked double maximum Prec peak as observed generally for the whole central Himalaya by Bookhagen and Burbank, 2006. In fact these author report for our specific case study (profiles 14 and 15 of their Fig.1(b)) a single step increase in relief associated with a single Prec maximum.”

Weak precipitation, warm winters and springs impact glaciers of south slopes of Mt. Everest (central Himalaya) in the last two decades (1994-2013)

Franco Salerno^(1,4*), Nicolas Guyennon⁽²⁾, Sudeep Thakuri^(1,4), Gaetano Viviano⁽¹⁾, Emanuele Romano⁽²⁾, Elisa Vuillermoz⁽⁴⁾, Paolo Cristofanelli^(3,4), Paolo Stocchi⁽³⁾, Giacomo Agrillo⁽³⁾, Yaoming Ma⁽⁵⁾, Gianni Tartari^(1,4)

⁽¹⁾ National Research Council, Water Research Institute, Brugherio (IRSA -CNR), Italy

⁽²⁾ National Research Council, Water Research Institute, Roma (IRSA-CNR), Italy

⁽³⁾ National Research Council, Institute of Atmospheric Sciences and Climate (ISAC-CNR) Bologna, Italy

⁽⁴⁾ Ev-K2-CNR Committee, Via San Bernardino, 145, Bergamo 24126, Italy

⁽⁵⁾ Institute of Tibetan Plateau Research, Chinese Academy of Science, China

**Correspondence to Franco Salerno*

Email: salerno@irsa.cnr.it

Address: IRSA-CNR Via Del Mulino 19. Località Occhiate 20861 Brugherio (MB)

Phone: +39 039 21694221

Fax: +39 039 2004692

Abstract

Studies on recent climate trends from the Himalayan range are limited, and even completely absent at high elevation (> 5000 m a.s.l.). This contribution specifically explores the southern slopes of Mt. Everest (central Himalaya), analyzing the minimum, maximum, and mean temperature and precipitation time series reconstructed from seven stations located between 2660 and 5600 m a.s.l. over the last twenty years (1994-2013). We complete this analysis with data from all the existing ground weather stations located on both sides of the mountain range (Koshi Basin) over the same period. Overall we observe that the main and more significant increase in temperature is concentrated outside of the monsoon period. ~~At higher elevations~~ Above 5000 m a.s.l. minimum temperature ($\pm 0.072 \pm 0.011$ °C $\text{a}^+ \text{y}^{-1}$, $p < 0.001$) increased far more than maximum temperature ($\pm 0.009 \pm 0.012$ °C $\text{a}^- \text{y}^{-1}$, $p > 0.1$), while mean temperature increased by $\pm 0.044 \pm 0.008$ °C $\text{a}^+ \text{y}^{-1}$, $p < 0.05$. Moreover, we note a substantial liquid precipitation weakening (-9.3 ± 1.8 mm $\text{a}^+ \text{y}^{-1}$, $p < 0.01$ during the monsoon season). The annual rate of decrease in precipitation at higher elevation is similar to the one at lower altitudes on the southern side of the Koshi Basin, but ~~here~~ the drier conditions of this remote environment make the fractional loss much more consistent (-47% during the monsoon period). This study contributes to change the perspective on which climatic driver (temperature vs. precipitation) led mainly the glacier responses in the last twenty years. The main implications are the following: 1) the negative mass balances of glaciers

observed in this region can be more ascribed to less accumulation due to weaker solid precipitation than to an increase of melting processes. 2) The melting processes have only been favored during winter and spring months and close to the glaciers terminus. 3) A decreasing of the probability of snowfall has significantly interested only the glaciers ablation zones (-10% , $p < 0.05$), but the magnitude of this phenomenon is decidedly lower than the observed decrease of precipitation. 4) The lesser accumulation could be the cause behind the observed lower glacier flow velocity and the current stagnation condition of tongues, which in turn could have triggered melting processes under the debris glacier coverage, leading to the formation of numerous supraglacial and proglacial lakes that have characterized the region in the last decades. Without demonstrating the causes that could have led to the climate change pattern observed at high elevation, we conclude -by listing the recent literature on hypotheses that accord with our observations.

Keywords: temperature lapse rate, precipitation gradient, monsoon weakening, Sequential Mann-Kendall, expectation maximization algorithm, climate change, glaciers shrinkage, central Himalaya

1 Introduction

The current uncertainties concerning the glacial shrinkage in the Himalayas are mainly attributed to a lack of measurements, both of the glaciers and of climatic forcing agents (e.g., Bolch et al., 2012). Recent results underline the need for a fine scale investigation, especially at high altitude, to better model the hydrological dynamics in this area. However, there are few high elevation weather stations in the world where the glaciers are located (Tartari et al., 2009). This can be attributed to the remote location of glaciers, the rugged terrain, and a complex political situation, all of which make physical access difficult (Bolch et al., 2012). As a consequence of the remoteness and difficulty in accessing many high elevation sites combined with the complications of operating automated weather stations (AWSs) at these altitudes, long-term measurements are challenging (Vuille, 2011). However, nearly all global climate models report increased sensitivity to warming at high elevations (e.g., Rangwala and Miller, 2012), while observations are less clear (Pepin and Lundquist, 2008). Moreover, changes in the timing or amount of precipitation are much more ambiguous and difficult to detect, and there is no clear evidence of significant changes in total precipitation patterns in most mountain regions (Vuille, 2011).

The need for a fine scale investigation is particularly evident on the south slope of Mt. Everest (central Southern Himalaya, CH-S) as it is one of the heavily glaciated parts of the Himalaya (Salerno et al., 2012; Thakuri et al., 2014). Nevertheless, these glaciers have the potential to build up moraine-dammed lakes storing large quantities of water, which are susceptible to GLOFs (glacial lake outburst floods) (e.g., Salerno et al., 2012; Fujita et al., 2013). Gardelle et al. (2011) noted that this region is most characterized by glacial lakes in the Hindu Kush Karakorum Himalaya. Recently, Thakuri et al. (2014)

noted that the Mt. Everest glaciers experienced an accelerated shrinkage in the last twenty years (1992-2011), as underlined by an upward shift of the Snow Line Altitude (SLA) with a velocity almost three times greater than the previous period (1962-1992). Furthermore Bolch et al. (2011) and Nuimura et al. (2012) found a higher mass loss rate during the last decade (2000–2010). Anyway, to date, there are not continuous meteorological time series able to clarify the causes of the melting process to which the glaciers of these slopes are subjected.

In this context, since the early 1990s, PYRAMID Observatory Laboratory (5050 m a.s.l.) was created by the *Ev-K2-CNR Committee* (www.ev-k2-cnr.org). This observatory is located at the highest elevation at which weather data has ever been collected in the region and thus represents a valuable dataset with which to investigate the climate change in CH-S (Tartari et al., 2002; Lami et al., 2010). However, the remoteness and the harsh conditions of the region over the years have complicated the operations of the AWSs, obstructing long-term measurements from a unique station.

In this paper, we mainly explore the small scale climate variability of the south slopes of Mt. Everest by analyzing the minimum, maximum, and mean air temperature (T) and liquid precipitation (Prec) time series reconstructed from seven AWSs located from 2660 to 5600 m a.s.l. over the last couple of decades (1994-2013). Moreover, we complete this analysis with all existing weather stations located on both sides of the Himalayan range (Koshi Basin) for the same period. In general, this study has the ultimate goal of linking the climate change patterns observed at high elevation with the glacier responses over the last twenty years, during which a more rapid glacier shrinkage process occurred in the region of investigation.

2 Region of investigation

The current study is focused on the Koshi (KO) Basin which is located in the eastern part of central Himalaya (CH) (Yao et al., 2012; Thakuri et al., 2014). To explore possible differences in the surroundings of Mt. Everest, we decided to consider the north and south parts of CH (with the suffixes -N and -S, respectively) separately (Fig. 1a). The KO River (58,100 km² of the basin) originates in the Tibetan Plateau (TP) and the Nepali highlands. The area considered in this study is within the latitudes of 27° and 28.5° N and longitudes of 85.5° and 88° E. The altitudinal gradient of this basin is the highest in the world, ranging from 77 to 8848 m a.s.l., i.e., Mt. Everest. We subdivide the KO Basin into the northern side (KO-N), belonging to the CH-N, and southern side (KO-S), belonging to the CH-S. The southern slopes of Mt. Everest are part of the Sagarmatha (Everest) National Park (SNP) (Fig. 1b), where the small scale climate variability at high elevation is investigated. The SNP is the world's highest protected area, with over 30000 tourists in 2008 (Salerno et al., 2010a; Salerno et al., 2013). The park area (1148 km²), extending from an elevation of 2845 to 8848 m a.s.l., covers the upper Dudh Koshi (DK) Basin (Manfredi et al., 2010; Amatya et al., 2010). Land cover classification shows that almost one-third of the territory is characterized by glaciers and ice cover (Salerno et al., 2008; Tartari et al., 2008), while less than 10% of the park

area is forested (Bajracharya et al., 2010; Salerno et al., 2010b). The SNP presents a broad range of bioclimatic conditions with three main bioclimatic zones: the zone of alpine scrub; the upper alpine zone, which includes the upper limit of vegetation growth; and the Arctic zone, where no plants can grow (UNEP and WCMC, 2008). Figure 1c shows the glacier distribution along the hypsometric curve of the SNP. We observe that the glacier surfaces are distributed from 4300 m to above 8000 m a.s.l., with more than 75% of the glacier surfaces lying between 5000 m and 6500 m a.s.l. The 2011 area-weighted mean elevation of the glaciers was 5720 m a.s.l. (Thakuri et al., 2014). These glaciers are identified as the summer accumulation-type fed mainly by summer Prec from the South Asian monsoon system, whereas the winter Prec caused by the mid-latitude westerly wind is minimal (Yao et al., 2012). The prevailing direction of the monsoons is S-N and SW-NE (e.g., Ichiyanagi et al., 2007). The climate is influenced by the monsoon system because the area is located in the subtropical zone with nearly 90% of the annual Prec falling in the months of June to September (this study). Heavy autumn and winter snowfalls can occur in association with tropical cyclones and westerly disturbances, respectively, and snow accumulation can occur at high elevations at all times of the year (Benn, 2012). Bollasina et al. (2002) have demonstrated the presence of well-defined local circulatory systems in the Khumbu Valley (SNP). The local circulation is dominated by a system of mountain and valley breezes. The valley breeze blows (approximately 4 m s^{-1}) from the south every day from sunrise to sunset throughout the monsoon season, pushing the clouds that bring Prec northward.

3 Data

3.1 Weather stations at high elevation

The first automatic weather station (named hereafter AWS0) at 5050 m a.s.l. near PYRAMID Observatory Laboratory (Fig. 1c), ~~and beginning was established~~ in October 1993, it has run continuously all year round (Bertolani et al., 2000). The station, operating in extreme conditions, had recorded long-term ground-based ~~meteorological temperature and temperature~~ data, ~~and the data which~~ are considered valid until December 2005. Due to the obsolescence of technology, the station was disposed of in 2006. A new station (named hereafter AWS1) was installed just a few tens of meters away from AWS0 and has been operating since October 2000. Other stations were installed in the following years in the upper DK Basin in the Khumbu Valley (Table 1). In 2008, the network included ~~the~~ sixth monitoring points, ~~including~~ the highest weather station of the world, located at South Col of Mt. Everest (7986 m a.s.l.). The locations of all stations are presented in Figure 1b. We can observe in Figure 1c that this meteorological network ~~represents well the climatic conditions~~ ~~represents the climatic conditions~~ of the SNP glaciers ~~well~~: AWS0 and AWS1 (5035 m a.s.l.) characterize the glacier fronts (4870 m a.s.l.), AWS4 (5600 m a.s.l.) represents the mean elevation of glaciers ~~in the~~

[area](#) (5720 m a.s.l.), and AWS5, the surface station at South Col (7986 m a.s.l.), characterizes the highest peaks (8848 m a.s.l.).

All stations, except AWS5 ([only T](#)), record at least T and Prec. This dataset presents some gaps (listed in Table 1) as a consequence of the complications of operating AWS at these altitudes. The list of measured variables for each stations and relevant data can be downloaded from <http://geonetwork.evkc2cnr.org/>. Data processing and quality checks are performed according to the international standards of the WMO (World Meteorological Organization).

The Prec sensors at these locations are [conventional heated](#) tipping buckets ~~usually used for rainfall measurements and which~~ may not fully capture the solid Prec. Therefore, [solid](#) Prec is probably underestimated, especially in winter. [However, in order to know the magnitude of the possible underestimation of the solid phase, we compared the monthly mean Prec of the reconstructed PYRAMID series \(1994-2013 period\) with the Prec of a station located downstream at 2619 m a.s.l. \(Chaurikhark, ID 1202\), \(Fig. 1b, Table 2\) which presents monthly mean temperature above 0 °C even during the winter and thus a high prevalence of liquid Prec also during these months. This comparison, supported by the elevated correlation existing between the monthly Prec of the two stations, shown a slight underestimation of the PYRAMID snow \(about 3±1% of total annual precipitation registered at PYRAMID, see Supplementary material 3 for more details\). Therefore, being much reduced the underestimation, we decided not to manipulate data. However the trends hereafter reported are referred mainly to the liquid phase of Prec.](#) In this regard, according to both Fujita and Sakai, 2014 and field observations (Ueno et al., 1994), the precipitation phase has been taken into account assuming that the probability of snowfall and rainfall depends on mean daily [air](#) temperature, using [as thresholds](#) – as proposed by the aforementioned authors – ~~as thresholds~~ 0 °C and 4 °C, respectively. In Figure 2 we first of all observe that at 5050 m a.s.l. 90% of precipitation is concentrated during June-September and that the probability of snowfall is very low (4%), considering that the mean daily temperature during these months is above 0 °C. On a yearly basis, this probability reaches 20% of the annual cumulated precipitation.

3.2 Other weather stations at lower altitude in the Koshi Basin

In KO-S Basin (Nepal), the stations are operated by the Department of Hydrology and Meteorology (DHM) (www.dhm.gov.np/). For daily T and Prec, we selected 10 stations for T and 19 stations for Prec considering both the length of the series and the monitoring continuity (< 10% of missing daily data). The selected stations cover an elevation range between 158 and 2619 m a.s.l. (Table 3). In KO-N Basin (TP, China), the number of ground weather stations (operated by the Chinese Academy of Science (CAS)), selected with the same criteria mentioned above, is considerably smaller, just two, but these stations have a higher elevation (4302 m [a.s.l.](#) for the Dingri station and 3811 m a.s.l. for the Nyalam station).

[The quality insurance of these meteorological data is ensured considering that they](#)

are used as part of global and regional networks including for instance APHRODITE (Asian Precipitation–Highly Resolved Observational Data Integration Towards Evaluation of Water Resources) (Yasutomi et al., 2011) and GHCN (Global Historical Climatology Network) (Menne et al., 2012).

4 Methods

We define the pre-monsoon, monsoon, and post-monsoon seasons as the months from February to May, June to September, and October to January, respectively. The minT, maxT, and meanT are calculated as the minimum, maximum, and mean daily air temperature. For total precipitation (Prec), we calculate the mean of the cumulative precipitation for the analyzed period.

4.1 Reconstruction of the daily temperature and precipitation time series at high elevation

The two stations named AWS0 and AWS1 in the last twenty years, considering the extreme weather conditions of ~~these slopes~~this area, present a percentage of missing daily values of approximately 20% (Table 1). The other stations (hereafter named secondary stations) were used here for infilling the gaps according to a priority criteria based on the degree of correlation among data. AWS1 was chosen as the reference station given the length of the time series and that it is currently still operating. Therefore, our reconstruction (hereafter named PYRAMID) is referred to an elevation of 5035 m a.s.l.

The selected infilling method is a simple regression analysis based on quantile mapping (e.g., Déqué, 2007; Themeßl et al., 2012). This ~~simple~~-regression method has been preferred to more complex techniques, such as the fuzzy rule-based approach (Abebe et al., 2000) or the artificial neural networks (Abudu et al., 2010; Coulibaly and Evora, 2007), considering the peculiarity of this case study. In fact, all stations are located in the same valley (Khumbu Valley). This aspect confines the variance among the stations to the altitudinal gradient of the considered variable (T or Prec), which can be easily reproduced by the stochastic link created by the quantile mapping method. In case all stations registered a simultaneous gap, we apply a multiple imputation technique (Schneider, 2001) that uses some other proxy variables to fill the remaining missing data. Details on the reconstruction procedure and the computation of the associated uncertainty are provided in Supplementary Material 1.

4.2 The trends analysis: the Sequential Mann-Kendall test

The Mann-Kendall (MK) test (Kendall, 1975) is widely adopted to assess significant trends in hydro-meteorological time series (e.g., Carraro et al., 2012a, 2012b; Guyennon et al., 2013). This test is non-parametric, thus being less sensitive to extreme sample values, and is independent of the hypothesis about the nature of the trend, whether

linear or not. The MK test verifies the assumption of the stationarity of the investigated series by ensuring that the associated normalized Kendall's tau coefficient, $\mu(\tau)$, is included within the confidence interval for a given significance level (for $\alpha = 5\%$, the $\mu(\tau)$ is below -1.96 and above 1.96). In the sequential form (seqMK) (Gerstengarde and Werner, 1999), $\mu(\tau)$ is calculated for each element of the sample. The procedure is applied forward starting from the oldest values (progressive) and backward starting from the most recent values (retrograde). If no trend is present, the patterns of progressive and retrograde $\mu(\tau)$ versus time (i.e., years) present several crossing points, while a unique crossing period allows the approximate location of the starting point of the trend (e.g., Bocchiola and Diolaiuti, 2010).

In this study, the seqMK is applied to monthly vectors. Monitoring the seasonal non-stationarity, the monthly progressive $\mu(\tau)$ is reported with a pseudo color code, where the warm colors represent the positive slopes and cold colors the negative ones. Color codes associated with values outside of the range (-1.96 to 1.96) possess darker tones to highlight the trend significance (Salerno et al., 2014). Moreover, to monitor the overall non-stationarity of the time series, both the progressive and the retrograde $\mu(\tau)$ at the annual scale are reported. We used the Sen's slope proposed by Sen (1968) as a robust linear regression allowing the quantification of the potential trends revealed by the seqMK (e.g., Bocchiola and Diolaiuti, 2010). The significance level is established for $p < 0.05$. We define a slight significance for $p < 0.10$. The uncertainty associated with the Sen's slopes (1994-2013) is estimated through a Monte Carlo uncertainty analysis (e.g., James and Oldenburg, 1997), described in detail in Supplementary Material 1.

5 Results

5.1 Trend analysis at high elevation

Figure 3 shows the reconstructed PYRAMID time series for minT, maxT, meanT, and Prec resulting from the overall infilling process explained in Supplementary Material 1. Figure 4 analyzes the monthly trends of T and Prec from 1994 to 2013 for PYRAMID.

Minimum air temperature (minT)

November (± 0.17 °C $\text{a}^{-1} \text{y}^{-1}$, $p < 0.01$) and December (± 0.21 °C $\text{a}^{-1} \text{y}^{-1}$, $p < 0.01$) present the highest increasing trend, i.e., both these two months experienced about even $+4$ °C over twenty years (Fig. 4a). In general, the post- and pre-monsoon periods experience higher and more significant increases than during the monsoon. In particular, we note the significant and consistent increase of minT of April (± 0.10 °C $\text{a}^{-1} \text{y}^{-1}$, $p < 0.05$). At the annual scale, the bottom graph shows a progressive $\mu(\tau)$ trend parallel to the retrograde $\mu(\tau)$ one for the entire analyzed period, i.e., a continuous tendency of minT to rise, which becomes significant in 2007, when the progressive $\mu(\tau)$ assumes values above $+1.96$. On the right, the Sen's slope completes the analysis, illustrating that

minT is increasing at annual level by $\pm 0.072 \pm 0.011$ °C $\text{a}^{-1} \text{y}^{-1}$, $p < 0.001$, i.e., $+1.44 \pm 0.22$ °C over twenty years.

Maximum air temperature (maxT)

The post- and pre-monsoon months show larger increases in maxT, but with lower magnitudes and significance than we observe for minT (Fig. 4b). The highest increases for this variable occurs also for ~~this variable~~ maxT in April, November and December. Less expected is the decrease of maxT in May (-0.08 °C $\text{a}^{-1} \text{y}^{-1}$, $p < 0.05$) and during the monsoon months from June to August (-0.05 °C $\text{a}^{-1} \text{y}^{-1}$, $p < 0.1$). On the annual scale, the bottom graph shows a continuous crossing of the progressive and retrograde $\mu(\tau)$ trends until 2007, i.e., a general stationary condition. From 2007 until 2010, the trend significantly increased, while 2012 and 2013 register a decrease, bringing the progressive $\mu(\tau)$ near the stationary condition. In fact, on the right, the Sen's slope confirms that maxT is at annual level stationary over the twenty years ($+0.009 \pm 0.012$ °C $\text{a}^{-1} \text{y}^{-1}$, $p > 0.1$).

Mean air temperature (meanT)

Figure 4c, as expected, presents intermediate conditions for meanT ~~than in respect to~~ ~~for~~ minT and maxT. All months, except May and the monsoon months from June and August, register a positive trend (more or less significant). December presents the highest a more significant increasing trend (± 0.17 °C $\text{a}^{-1} \text{y}^{-1}$, $p < 0.01$), while April shows the highest and a more significant increase ($p < 0.10$) during the pre-monsoon period. On the annual scale, the bottom graph shows that the progressive $\mu(\tau)$ trend has always increased since 2000 and that it becomes significant beginning in 2008. On the right, the Sen's slope concludes this analysis, showing that meanT has been significantly increasing by $\pm 0.044 \pm 0.008$ °C $\text{a}^{-1} \text{y}^{-1}$, $p < 0.05$, i.e., $+0.88 \pm 0.16$ °C over twenty years.

Total precipitation (Prec)

In the last years, all cells are blue, i.e., we observe for all months an overall and strongly significant decreasing trend of Prec (Fig. 4d). In general, the post- and pre-monsoon periods experience more significant decreases, although the monsoon months (June-September) register the main Prec losses (e.g. August registers a Prec loss of even -4.6 mm $\text{a}^{-1} \text{y}^{-1}$). On the annual scale, the bottom graph shows a continuous decreasing progressive $\mu(\tau)$ trend since 2000 that becomes significant beginning in 2005. On the right, the Sen's slope notes that the decreasing Prec trend is strongly high and significant at annual level (-13.7 ± 2.4 mm $\text{a}^{-1} \text{y}^{-1}$, $p < 0.001$).

The precipitation reduction is mainly due to a reduction in intensity (cumulative precipitation for week). However during the early and late monsoon rather show a reduction in duration (number of we days for week) (see further details in Supplementary Material 2).

5.2 Trend analysis in the Koshi Basin

Table 2 provides the descriptive statistics of the Sen's slopes for minT, maxT, meanT, and Prec for the 1994-2013 period for the Koshi Basin. The stations located on the two sides of the Himalayan range are listed separately. For the southern ones (KO-S), we observe that for minT less than half of the stations experience an increasing trend and just three are significant with $p < 0.1$. In general, the minT on the southern side can be defined as stationary ($+0.003\text{ }^{\circ}\text{C a}^{-1}\text{ y}^{-1}$). Conversely, the maxT shows a decidedly non-stationary condition. All stations present an increasing trend, and even six of the ten are on the significant rise with at least $p < 0.1$. The mean trend is $+0.060\text{ }^{\circ}\text{C a}^{-1}\text{ y}^{-1}$ ($p < 0.10$). Similarly, the meanT shows a substantial increase. Also in this case, six of the ten stations are on the significant rise with at least $p < 0.1$. The mean trend is $+0.029\text{ }^{\circ}\text{C a}^{-1}\text{ y}^{-1}$ ($p < 0.10$). In regards to Prec, we observe that on the KO-S, 14 of the 19 stations present a downward trend. Among them, eight decrease significantly with at least $p < 0.1$. The mean trend is $-11.1\text{ mm a}^{-1}\text{ y}^{-1}$, i.e., we observe a decreasing of 15% (222 mm) of precipitation fallen in the basin during the 1994-2013 period (1527 mm on average).

The two stations located on the northern ridge (KO-N) show a singularly slight significant rise for minT ($\pm 0.034\text{ }^{\circ}\text{C a}^{-1}\text{ y}^{-1}$, $p < 0.10$ on average) and for maxT ($\pm 0.039\text{ }^{\circ}\text{C a}^{-1}\text{ y}^{-1}$, $p < 0.10$ on average), recording a consequent mean increase of meanT equal to $\pm 0.037\text{ }^{\circ}\text{C a}^{-1}\text{ y}^{-1}$, $p < 0.05$. As for Prec, we observe that on the KO-N both stations maintain stationary conditions ($-0.1\text{ mm a}^{-1}\text{ y}^{-1}$).

Table 3 provides the descriptive statistics of the Sen's slopes on a seasonal base. The stations analyzed here are the same as those considered in Table 2. We begin our description with PYRAMID, already analyzed in detail in Figure 4. We confirm with this seasonal grouping that the main and significant increases of minT, maxT, and meanT are completely concentrated during the post-monsoon period (e.g., $\pm 0.124\text{ }^{\circ}\text{C a}^{-1}\text{ y}^{-1}$, $p < 0.01$ for meanT). The pre-monsoon period experienced a slighter and not significant increase (e.g., $\pm 0.035\text{ }^{\circ}\text{C a}^{-1}\text{ y}^{-1}$, $p > 0.1$ for meanT). In general, during the monsoon period, T is much more stationary for all three variables (e.g., $\pm 0.015\text{ }^{\circ}\text{C a}^{-1}\text{ y}^{-1}$, $p > 0.1$ for meanT). Considering the other KO-S stations, the main increasing and significant trends of meanT occurred during the pre-monsoon ($\pm 0.043\text{ }^{\circ}\text{C a}^{-1}\text{ y}^{-1}$) and post-monsoon ($\pm 0.030\text{ }^{\circ}\text{C a}^{-1}\text{ y}^{-1}$) season, while the increase during the monsoon is slighter ($\pm 0.020\text{ }^{\circ}\text{C a}^{-1}\text{ y}^{-1}$). The KO-N stations confirm that the main increasing trend of meanT occurred outside the monsoon period that is stationary ($+0.013\text{ }^{\circ}\text{C a}^{-1}\text{ y}^{-1}$).

As for Prec, PYRAMID and the other KO-S stations show that the magnitude of the Sen's slopes is higher during the monsoon season ($-9.3\text{ mm a}^{-1}\text{ y}^{-1}$ and $-8.6\text{ mm a}^{-1}\text{ y}^{-1}$, respectively), when precipitation is more abundant. The relatively low snowfall phase of monsoon Prec at PYRAMID (as specified above) makes the decreasing trend observed during the summer more robust than the annual one as devoid of ~~possible-the~~ undervaluation of snowfall, although slight as demonstrated above ($3\pm 1\%$). The northern stations show slight significant decreasing Prec during the winter ($-3.3\text{ mm a}^{-1}\text{ y}^{-1}$, $p < 0.05$).

5.3 Lapse rates in the southern Koshi Basin

5.3.1 Air temperature gradient

This study, aiming to create a connection between the climate drivers and cryosphere in the Koshi Basin, which presents the highest altitudinal gradient of the world (77 to 8848 m a.s.l.), offers a unique opportunity to calculate T and Prec lapse rates before analyzing their spatial trends. It is worth noting that the T lapse rate is one of the most important variables for modeling meltwater runoff from a glacierized basin using the T-index method (Hock, 2005; Immerzeel et al., 2014). It is also an important variable for determining the form of Prec and its distribution characteristics (e.g., Hock, 2005). Figure 5a-5b presents the lapse rate of the annual mean T in the KO Basin (Nepal) along the altitudinal range of well over 7000 m (865 to 7986 m a.s.l.). We found an altitudinal gradient of $-0.60\text{ }^{\circ}\text{C (100 m)}^{-1}$ on the annual scale with a linear trend ($r^2 = 0.98$, $p < 0.001$). It is known that up to altitudes of approximately 8-17 km a.s.l. in the lower regions of the atmosphere, T decreases with altitude at a fairly uniform rate (Washington and Parkinson, 2005). ~~Kattel and Yao (2013) recently found a lower annual lapse rate for the overall CH-S, but until 4000 m a.s.l.: $-0.52\text{ }^{\circ}\text{C (100 m)}^{-1}$.~~

Considering that the lapse rate is mainly affected by the moisture content of the air (Washington and Parkinson, 2005), we ~~also~~ calculated the seasonal gradients (not shown here). We found a dry lapse rate of $-0.65\text{ }^{\circ}\text{C (100 m)}^{-1}$ ($r^2 = 0.99$, $p < 0.001$) during the pre-monsoon season when AWS1 registers a mean relative humidity of 62%. A saturated lapse rate during the monsoon season is $-0.57\text{ }^{\circ}\text{C (100 m)}^{-1}$ ($r^2 = 0.99$, $p < 0.001$) with a mean relative humidity of 96%. During the post-monsoon period, we found a lapse rate equal to that registered during the monsoon: $-0.57\text{ }^{\circ}\text{C (100 m)}^{-1}$ ($r^2 = 0.98$, $p < 0.001$) even if the relative humidity is decidedly lower in these months (44%). Kattel and Yao (2013) explain this anomalous low post-monsoon lapse rate as the effect of strong radiative cooling in winter.

5.3.2 Precipitation gradient

~~The relationship of Prec with elevation helps in. As for Prec, its relationship with elevation helps in~~ providing a realistic assessment of water resources and hydrological modeling of mountainous regions (Barros et al., 2004). In recent years, the spatial variability of Prec has received attention because the mass losses of the Himalayan glaciers can be explained with an increased variability in the monsoon system (e.g., Yao et al., 2012; Thakuri et al., 2014). ~~Some previous studies of the Himalayas have considered orographic effects on Prec (Singh and Kumar, 1997; Ichihyanagi et al., 2007). Ichihyanagi et al. (2007), using all available Prec stations operated by DHM, of which 5% of stations are located over 2500 m and just one station is over 4000 m a.s.l., observed that in the CH-S region, the annual Prec increases with altitude below 2000 m a.s.l. and decreases for elevations ranging between 2000 and 3500 m a.s.l., but with no significant gradient. A broad picture of the relationship between Prec and topography in~~

~~the Himalayas can be derived from the precipitation radar onboard the Tropical Rainfall Measuring Mission (TRMM). Some authors found an increasing trend with elevation characterized by two distinct maxima along two elevation bands (950 and 2100 m a.s.l.). The second maximum is much higher than the first, and it is located along the Lesser Himalayas. Over these elevations, the annual distribution follows an approximate exponentially decreasing trend (Bookhagen and Burbank, 2006).~~

Figure 5^{ab} shows the altitudinal gradient for the total annual Prec in the Koshi Basin. We observe a clear rise in Prec with elevation until approximately 2500 m a.s.l., corresponding to the Tarke Ghyang station (code 1058), registering an annual mean of 3669 mm (mean for the 2004-2012 period). A linear approximation ($r = 0.83$, $p < 0.001$) provides a rate of $+1.16 \text{ mm m}^{-1}$. At higher elevations, we observe an exponential decrease (ae^{bx} , with $a = 21168 \text{ mm m}^{-1}$ and $b = -9 \cdot 10^{-4} \text{ m}^{-1}$, where x is the elevation expressed as m a.s.l.) until observing a minimum of 132 mm (years 2009 and 2013) for the Kala Patthar station (AWS4) at 5600 m a.s.l., although, as specified above, at these altitudes the contribution of winter snowfall could be slightly underestimated. The changing point between the two gradients can be reasonably assumed at approximately 2500 m a.s.l., considering that the stations here present the highest interannual variability, belonging in this way, depending on the year, to the linear increase or to the exponential decrease. The clear outlier along the linear gradient is the Num Station (1301) located at 1497 m a.s.l., which recorded 4608 mm of precipitation. This station has been excluded for the linear approximation because, as reported by Montgomery and Stolar (2006), the station is located in the Arun Valley, which acts as a conduit for northward transport of monsoonal precipitation. The result is that local precipitation within the gorge of the Arun River is several times greater than in surrounding areas.

Some previous studies of the Himalayas have considered orographic effects on Prec (Singh and Kumar, 1997; Ichiyanagi et al., 2007). Ichiyanagi et al. (2007), using all available Prec stations operated by DHM, of which $< 5\%$ of stations are located over 2500 m and just one station is over 4000 m a.s.l., observed that in the CH-S region, the annual Prec increases with altitude below 2000 m a.s.l. and decreases for elevations ranging between 2000 and 3500 m a.s.l., but with no significant gradient. A broad picture of the relationship between Prec and topography in the Himalayas can be derived from the precipitation radar onboard the Tropical Rainfall Measuring Mission (TRMM). Some authors found an increasing trend with elevation characterized by two distinct maxima along two elevation bands (950 and 2100 m a.s.l.). The second maximum is much higher than the first, and it is located along the Lesser Himalayas. Over these elevations, the annual distribution follows an approximate exponentially decreasing trend (Bookhagen and Burbank, 2006).

Physically, we can interpret the Prec gradient of Fig. 5a considering that when the humid air masses coming from the Bay of Bengal collide with the orographic barrier, heavy convections induce huge quantity of rain below 2500 m a.s.l.. The topographic barrier of the Himalayan mountain range causes the mechanical lift of the humid air, the cooling of the air column, the condensation and the consequent rainfall. The further

increase in relief induces a depletion of the moisture content resulting in a severe reduction of Prec at higher altitudes. Our study, based on ground stations, confirms the general Prec gradient detected with the TRMM microwave observations, even if we did not identified a marked double maximum Prec peak as observed generally for the whole central Himalaya by Bookhagen and Burbank, 2006. In fact these author report for our specific case study (profiles 14 and 15 of their Fig.1(b)) a single step increase in relief associated with a single Prec maximum.

5.4 Spatial distribution of air temperature and precipitation trends in the Koshi Basin

Figure 6 presents the spatial distribution of the Sen's slopes in the Koshi Basin for minT (Fig. 6a), maxT (Fig. 6b), meanT (Fig. 6c), and Prec (Fig. 6d) during the 1994-2013 period. The relevant data are reported in Table 2. The Chainpur (East) station shows T trends in contrast with the other stations (see also Table 2); therefore, we consider this station as a local anomaly and do not discuss it further in the following sections.

In regards to minT, we observe an overall stationary condition in KO-S, as noted above. The only two stations showing a significant increasing trend are both located at East. The high elevation stations (PYRAMID and both those located on the north ridge) differ from the general pattern of the southern basin by showing a significant increasing trend. Even for maxT, we observe a higher increase in the southeastern basin. The central and western parts of the KO-S seem to be more stationary. PYRAMID follows this stationary pattern, while the northern stations (KO-N) show large and significant increases. As a consequence, meanT shows increasing trends for all the Koshi Basin, especially on the southeast and northern sides.

The decrease of precipitation in the southern Koshi Basin presents a quite homogeneous pattern from which the highly elevated PYRAMID is not excluded. The pattern is different on the north ridge, where it is stationary.

6 Discussion

6.1 Temperature trends of the Koshi Basin compared to the regional pattern

The trend analysis carried out in this study for the last two decades in KO-S shows full consistency with the pattern of change (shown in the following) occurring in these regions over the last three decades in terms of a higher increase in maxT (+0.060 °C y⁻¹) than in minT (+0.003 °C y⁻¹), a seasonal pattern (more pronounced during the pre- and post-monsoon months), and the magnitudes of the trends (e.g., the meanT trend is +0.030 °C y⁻¹). Therefore, at low elevations of KO-S, we observe an acceleration of warming in the recent years compared to the rate of change reported by Kattel and Yao (2013) and Shrestha et al. (1999) in the previous decades.

At regional level, Kattel and Yao (2013) analyzed the annual minT, maxT, and meanT trends from stations ranging from 1304 m to 2566 m a.s.l. in CH-S (corresponding to all stations in Nepal) during the 1980–2009 period. They found that the magni-

tude of warming is higher for maxT ($\pm 0.065^{\circ}\text{C a}^{-1}\text{y}^{-1}$), while minT ($\pm 0.011^{\circ}\text{C a}^{-1}\text{y}^{-1}$) exhibits larger variability, such as positive, negative or no change; meanT was found to increase at an intermediate rate of $\pm 0.038^{\circ}\text{C a}^{-1}\text{y}^{-1}$. These authors extended some time series and confirmed the findings of Shrestha et al. (1999) that, analyzing the 1971–1994 period, found a maxT increase of $\pm 0.059^{\circ}\text{C a}^{-1}\text{y}^{-1}$ for all of Nepal. Furthermore, warming in the winter was more pronounced compared to other seasons in both studies. These results are consistent with the pattern reported in WH (e.g., Bhutiyani et al., 2007; Shekhar et al., 2010), in EH, and in the rest of India (e.g., Pal and Al-Tabbaa, 2010) for the last three decades.

~~The trend analysis carried out in this study for the last two decades in KO-S shows full consistency with the pattern of change occurring in these regions over the last three decades in terms of a higher increase in maxT ($0.060^{\circ}\text{C a}^{-1}$) than in minT ($0.003^{\circ}\text{C a}^{-1}$), a seasonal pattern (more pronounced during the pre and post monsoon months), and the magnitudes of the trends (e.g., the meanT trend is $+0.030^{\circ}\text{C a}^{-1}$). Therefore, at low elevations of KO-S, we observe an acceleration of warming in the recent years compared to the rate of change reported by Kattel and Yao (2013) and Shrestha et al. (1999) in the previous decades.~~

The trend analysis carried out in this study for the last two decades in KO-N agrees with the regional studies (shown in the following) in regards to both the considerable increase of minT ($+0.034^{\circ}\text{C y}^{-1}$) and the seasonal consistency of trends, related to all three T variables, outside the monsoon months. However, we observe that in recent years, maxT is increasing more than the rest of the TP ($+0.039^{\circ}\text{C y}^{-1}$). In general we observed an increase of meanT ($0.037^{\circ}\text{C y}^{-1}$) comparable to that reported by Yang et al. (2012) ($0.031^{\circ}\text{C y}^{-1}$) in the 1971–2007 period.

~~At regional level, Different conditions have been observed on the TP, where the warming of minT is more prominent than that of maxT (e.g., Liu et al., 2006; Liu et al., 2009). In particular, for stations above 2000 m a.s.l. during the 1961–2003 period, Liu et al. (2006) found that minT trends were consistently greater ($+0.041^{\circ}\text{C a}^{-1}\text{y}^{-1}$) than those of maxT ($+0.018^{\circ}\text{C a}^{-1}\text{y}^{-1}$), especially in the winter and spring months. Yang et al. (2012), focusing their analysis on CH-N (which corresponds to the southern TP) in a more recent period (1971–2007), showed a significant increase of $\pm 0.031^{\circ}\text{C a}^{-1}\text{y}^{-1}$ for meanT. Yang et al. (2006) analyzed five stations located in a more limited area of CH-N: the northern side of Mt. Everest (therefore, including the two stations also considered in this study) from 1971 to 2004. The warming is observed to be influenced more markedly by the minT increase.~~

~~The trend analysis carried out in this study for KO-N over the last two decades agrees with these studies in regards to both the considerable increase of minT ($0.034^{\circ}\text{C a}^{-1}$) and the seasonal consistency of trends, related to all three T variables, outside the monsoon months. However, we observe that in recent years, maxT is increasing more than the rest of the TP ($0.039^{\circ}\text{C a}^{-1}$). In general we observed an increase of meanT ($0.037^{\circ}\text{C a}^{-1}$) comparable to that reported by Yang et al. (2012) ($0.031^{\circ}\text{C a}^{-1}$) in the 1971–2007 period.~~

~~With all these regional studies, Summarizing~~ PYRAMID shares the higher T trends outside the monsoon period. However, in contrast with studies located south of the Himalayan ridge, which observed a prevalence of maxT increase, PYRAMID experienced a consistent minT increase ($\pm 0.072\text{ }^{\circ}\text{C a}^{-1}\text{y}^{-1}$ for PYRAMID vs $\pm 0.003\text{ }^{\circ}\text{C a}^{-1}\text{y}^{-1}$ for KO-S stations), while the maxT increase is decidedly weaker ($\pm 0.009\text{ }^{\circ}\text{C a}^{-1}\text{y}^{-1}$ for PYRAMID vs $\pm 0.060\text{ }^{\circ}\text{C a}^{-1}\text{y}^{-1}$ for KO-S stations). The remarkable minT trend of PYRAMID is higher, but more similar to the pattern of change commonly described on the TP, in particular in CH-N, and also in this study ($\pm 0.072\text{ }^{\circ}\text{C a}^{-1}\text{y}^{-1}$ for PYRAMID vs $\pm 0.034\text{ }^{\circ}\text{C a}^{-1}\text{y}^{-1}$ for KO-N stations), while the maxT increase is weaker ($\pm 0.009\text{ }^{\circ}\text{C a}^{-1}\text{y}^{-1}$ for PYRAMID vs $\pm 0.039\text{ }^{\circ}\text{C a}^{-1}\text{y}^{-1}$ for KO-N stations).

6.2 Elevation dependency of temperature trends

Figure 7 shows T trends in the KO Basin for minT, meanT, and maxT relative to the elevation during the 1994-2013 period. No linear pattern emerges. However, we can observe the minT trend of the three stations located at higher altitude (PYRAMID and KO-N stations), which increases more than that of the lower stations (Fig. 7a, see also Table 2). Reviewing the most recent studies in the surroundings, we found that they are quite exclusively located on CH-N. These studies often show contradictory elevation dependencies (Rangwala and Miller, 2012). A recent study by You et al. (2010) did not find any significant elevation dependency in the warming rates of meanT between 1961 and 2005. However, considering mostly the same stations, Liu et al. (2009) found that the warming rates for minT were greater at higher elevations. Observations from CH-S are much rarer. Shrestha et al. (1999) found elevation dependency in the rate at which maxT were increasing in the Nepali Himalayas (CH-S), with higher rates at higher elevations, but this study exclusively considered stations under 3000 m a.s.l.

Furthermore we did not find for the Koshi Basin any significant elevation dependency in the weakening rates of Prec.

6.3 Precipitation trends of the Koshi Basin compared to the regional pattern

As will be detailed in the following, different from the north side of Mt. Everest and from the general TP, we confirm the general monsoon weakening in the KO-S, observing a substantial Prec decrease of 15% (-11.1 mm y⁻¹, -222 mm), but that is not significant for all stations. At PYRAMID, the annual loss is relatively comparable with that of the KO-S (-13.7 mm y⁻¹, -273 mm), but at these high elevations, as we observed in Table 2, the weather is much more drier (449 and 1527 mm, respectively). Therefore, the fractional loss is more than 3 times (-52%) that of the KO-S. Considering that the decreasing trend observed during the summer is more robust than the annual one (see above), the fractional loss of Prec during the monsoon is -47%, which means that currently, on average, the precipitation at PYRAMID is the half of what it was twenty years ago.

At regional level, Turner and Annamalai (2012), using the all-India rainfall data based on a weighted mean of 306 stations, observed a negative precipitation trend since the 1950s in South Asia. According to Yao et al. (2012), using the Global Precipitation Climatology Project (GPCP) data, there is strong evidence that precipitation from 1979 to 2010 decreased even in the Himalayas. In eastern CH-S, where the Koshi Basin is located, they estimated a loss of 173 mm, showing a real decreasing trend starting from the early 1990s (mean value between grid 9 and 11 in Fig. S18 of their paper).

On the TP, the observed pattern of change is opposite that of the monsoon weakening described by the authors cited above. Liu et al. (2010) described an increase in precipitation in CH-N for the period of the 1980s to 2008. Su et al. (2006) described a marked precipitation increase in the Yangtze River Basin (eastern CH-N). In a similar way to the T analysis, Yang et al. (2006) considered 5 stations located on the northern side of Mt. Everest (therefore, including the two stations also considered in this study) from 1971 to 2004 and observed an increasing, but not significant Prec trend. The higher stationarity we observed is confirmed since 1971 for the two KO-N stations considered in this study.

~~Different from the north side of Mt. Everest and from the general TP, we confirm the general monsoon weakening in the KO-S, observing a substantial Prec decrease of 15% (-11.1 mm a^{-1} , 222 mm), but that is not significant for all stations. At PYRAMID, the annual loss is relatively comparable with that of the KO-S (13.7 mm a^{-1} , 273 mm), but at these high elevations, as we observed in Table 2, the weather is much more drier (449 and 1527 mm, respectively). Therefore, the fractional loss is more than 3 times (52%) that of the KO-S. Considering that the decreasing trend observed during the summer is more robust than the annual one (see above), the fractional loss of Prec during the monsoon is 47%, which means that currently, on average, the precipitation at PYRAMID is the half of what it was twenty years ago.~~

6.4 Mechanisms responsible for temperature warming and precipitation weakening

According to Rangwala and Miller (2012), there are a number of mechanisms that can cause enhanced warming rates at high elevation, and they often have strong seasonal dependency. These mechanisms arise from either elevation based differential changes in climate drivers, such as snow cover, clouds, specific humidity, aerosols, and soil moisture, or differential sensitivities of surface warming to changes in these drivers at different elevations. This study does not aim to either realize a comprehensive review or to demonstrate the causes that could have led to the climate change pattern observed at PYRAMID, but our intent here is just to note the recent hypotheses advanced in the literature that fit with our observations for the region of investigation.

Snow/ice albedo is one of the strongest feedbacks in the climate system (Rangwala and Miller, 2012). Increases in minT are possible if decreases in snow cover are accompanied by increases in soil moisture and surface humidity, which can facilitate a greater diurnal retention of the daytime solar energy in the land surface and amplify the

longwave heating of the land surface at night (Rangwala et al., 2012). For the Tibetan Plateau, Rikiishi and Nakasato (2006) found that the length of the snow cover season declined at all elevations between 1966 and 2001. Moreover, minT can be enhanced by nighttime increases in cloud cover. However, assessing changes in clouds and quantifying cloud feedbacks will remain challenging in the near term. For the Tibetan Plateau, Duan and Wu (2006) found that low level nocturnal cloud cover increased over the TP between 1961 and 2003 and that these increases explain part of the observed increases in minT.

The maxT increase observed here during April ($p < 0.05$ in 2011, Fig. 4b) fits with the warming reported by Pal and Al-Tabbaa (2010) which observed that within the pre-monsoon season only April shows significant changes in maxT in all Indian regions and WH (1901-2003 period). According to Ramanathan et al. (2007), Gautam et al. (2010) argued that the observed warming during the pre-monsoon period (April-June) can be ascribed not only to the global greenhouse warming, but also to the solar radiation absorption caused by the large amount of aerosol (mineral dust mixed with other carbonaceous material) transported over the Gangetic-Himalayan region. As recently reported by Marinoni et al. (2013), April represents the month for which the transport of absorbing carbonaceous aerosol (i.e. black carbon) is maximized in our region of investigation (Khumbu Valley). At this regards Putero et al. (2013) show evidences for a possible influence of open fire occurrence in South Asia particular abundant during this period of the year. However the significant decreasing of maxT observed in May ($p < 0.05$) and the slight significant decreasing during the monsoon months from June to August ($p < 0.10$) appear to deviate from the scenario proposed for April. In this respect it should be kept in mind that the radioactive dynamical interactions of aerosol with the monsoon cycle are extremely complex and different processes can interact with each other. As an instance, as reported by Qian et al. (2011), the deposition of absorbing aerosol on snow and the snow albedo feedback processes can play a prominent role in Himalayas and TP inducing large radioactive flux changes and surface temperature perturbation.

Recent studies associate the precipitation decrease over India during the second half of 20th century (e.g., Ramanathan et al., 2005; Lau and Kim, 2006) to the significant tropospheric warming over the tropical area from the Indian Ocean to the western Pacific (e.g., Wu, 2005), while westerlies are strengthening (Zhao et al., 2012). Other authors (e.g., Bollasina et al., 2011) attribute the monsoon weakening to human-influenced aerosol emissions. In fact an increase of aerosols over South Asia has been well documented (Ramanathan et al., 2005; Lau and Kim, 2006) and climate model experiments suggest that sulfate aerosol may significantly reduce monsoon precipitation (Mitchell and Johns, 1997). Despite a historical weakening of the monsoon circulation, most studies project an increase of the seasonal monsoon rainfall under global warming. At this regards Levy II et al., 2013 find that the dramatic emission reductions (35%–80%) in anthropogenic aerosols and their precursors projected by Representative Concentration Pathway (RCP) 4.5 (Moss et al., 2010) result an increasing trend by the second half of the 21st century in South Asia and in particular over the Himalaya

(Palazzi et al., 2013).

6.5 Linking climate change patterns observed at high elevation with glacier responses

6.5.1 Impact of temperature increase

Air temperature and precipitation are the two factors most commonly related to glacier fluctuations. However, there still exists a seasonal gap in order to explain the shrinking of summer accumulation-type glaciers (typical of CH) due to large temperature increases observed in the region during winter (Ueno and Aryal, 2008), as is the case for the south slopes of Mt. Everest. Furthermore, in this study we noted a slightly significant decline in summer maxT and stationary meanT. The real increase of T has been observed for minT, but given the mean elevation of glaciers (5695 m a.s.l. in 1992) and the mean elevation range of glacier fronts (4568-4817 m a.s.l. in 1992, mean 4817 m a.s.l., 249 m of standard deviation –sd-) (Thakuri et al., 2014), this increase for minT can be most likely considered ineffective for melting processes, since T is still less than 0 °C. This inference can be ascertained analyzing Figure 8, created in order to link temperature increases and altitudinal glacier distribution (data from Thakuri et al., 2014). The 0 °C isotherms, corresponding to the mean monthly minT and maxT, are plotted for 1994 and 2013. The elevation of each 0 °C isotherm is calculated according to the accurate lapse rates computation carried out in this study and the observed monthly T trends. We can note that in 1994 the 0 °C isotherm for minT reached the elevation band characterizing the glacier fronts only from June to September. However, twenty years later, the upward of the 0 °C isotherm is modest (± 92 m) during these months, compared to the huge but ineffective rise for melting processes (downstream from the glacier fronts) of December-November (even ± 854 m). The maxT has obviously a greater potential impact on glaciers. In fact the 0 °C isotherm for of all months except January and February crosses the elevation bands within which the glacier fronts are located ever since 1994. In this regard we observe that only April (± 224 m), December (± 212 m), and November (± 160 m) experienced an upward of the 0 °C isotherm able to enhance the melting processes, but only close to the glaciers fronts. We therefore point out that the impact caused by the increased temperature occurring in April most likely plays an important role not only in relation to this case study, but also at the level of the Himalayan range. In fact, as mentioned above, Pal and Al-Tabbaa (2010), observed that within the pre-monsoon season, only April showed significant changes in maxT in all Indian regions and WH (1901-2003 period).

6.5.2 Impact of precipitation decrease

As regards the precipitation, in this study we noted a strong and significant decreasing Prec trend for all months, corresponding to a fractional loss of 47% during the monsoon season which indicates that, on average, the precipitation at PYRAMID is currently half of what it was twenty years ago. This climate change pattern confirms and

clarifies the observation of Thakuri et al. (2014), who noted that the southern Mt. Everest glaciers experienced a shrinkage acceleration over the last twenty years (1992–2011), as underlined by an upward shift of SLA with a velocity almost three times greater than the previous period (1962–1992). The authors, without the support of climatic data, proposed the hypothesis that Mt. Everest glaciers are shrinking faster since the early 1990s mainly as a result of a weakening of precipitation over the last decades. In fact they observed a double upward shift in the SLA of the largest glaciers (south-oriented and with a higher altitude accumulation zone): a clear signal of a significant decrease in accumulation. Wagnon et al. (2013) have recently reached the same conclusion, but also in this case without the support of any climatic studies. Bolch et al. (2011) and Nuimura et al. (2012) registered a higher mass loss rate during the last decade (2000–2010).

Furthermore Quincey et al. (2009) and Peters et al. (2010) observed lower glacier flow velocity in the region over the last decades. Many studies highlight how the present condition of ice stagnation of glaciers in the Mt Everest region, and in general in CH-S, is attributable to low flow velocity generated by generally negative mass balances (Bolch et al., 2008; Quincey et al., 2009; Scherler et al., 2011). Our observations allow attributing the lower glacier flow velocity to lower accumulation due to weaker precipitation, which can thus be considered the main climatic factor driving the current ice stagnation of tongues. In this regard we need to keep in mind that changes in velocity are among the main triggers for the formation of supraglacial and proglacial lakes (Salerno et al., 2012; Quincey et al., 2009), which we know to be susceptible to GLOFs.

6.5.3 Trend analysis of annual probability of snowfall

Figure 9 analyses how the changes observed for the meanT at PYRAMID have affected the probability of snowfall on total cumulated annual precipitation in the last twenty years. The increase of meanT observed outside the monsoon period, when the precipitation is almost completely composed by snow (Fig. 2), brought a significant decrease of solid phase ($+0.7\% \text{ a}^{-1} \text{ y}^{-1}$, $p < 0.05$). Extending this analysis to the elevation bands characterizing the glaciers distribution (see Fig. 8), through the temperature lapse rate calculated here, we observe that at the level of the mean glaciers (5695 m a.s.l.) the probability of snowfall is stationary ($+0.04\% \text{ a}^{-1} \text{ y}^{-1}$), while it decreases at the mean elevation of SLAs (5345 m a.s.l. in 1992, Thakuri et al., 2014), but not significantly ($-0.38\% \text{ a}^{-1} \text{ y}^{-1}$, $p > 0.1$). The reduction becomes significant at lower altitudes. In particular, at the mean elevation of glacier fronts (4817 m a.s.l.) the probability of snowfall is $-0.56\% \text{ a}^{-1} \text{ y}^{-1}$ ($p < 0.05$), i.e. at these altitudes the probability of snow on annual base is currently 11 % ($p < 0.05$) less than twenty years ago. We can conclude this analysis summarizing that a significant change in precipitation phase has occurred close to the terminal portions of glaciers, corresponding broadly to the glaciers ablation zones (around 10 %, $p < 0.5$), while the lower temperature of the upper glaciers zones

has so far guaranteed a stationary condition.

Conclusion

Most relevant studies on temperature trends were conducted on the Tibetan Plateau, the Indian subcontinent (including the WH) and the Upper Indus Basin, while studies on the mountainous regions along the southern slope of the central Himalayas in Nepal (CH-S) are limited. Although Shrestha et al. (1999) analyzed the maximum temperature trends over Nepal during the period 1971–1994, studies on recent temperature trends over CH-S are still lacking and, before this study, completely absent as regards high elevation. This paper addresses seasonal variability of minimum, maximum, and mean temperatures and precipitation at high elevation on the southern slopes of Mt. Everest. Moreover, we complete this analysis with data from all the existing weather stations located on both sides of the Himalayan range (Koshi Basin) for the 1994–2013 period, during which a rapid glacier mass loss occurred.

At high elevation on the southern slopes of Mt. Everest, we observed the following:

- 1) The main increases in air temperature are almost completely concentrated during the post-monsoon months. The pre-monsoon period experienced a slighter and insignificant increase, while the monsoon season is generally stationary. This seasonal temperature change pattern is shared with the entire Koshi Basin, and it is also observed in the regional studies related to the northern and southern slopes of the Himalayan range. Surprisingly, ~~at high elevation~~above 5000 m a.s.l. the maximum temperature decreases significantly in May and slightly during the monsoon months from June to August.
- 2) The minimum temperature increased much more than the maximum temperature. This remarkable minimum temperature trend is more similar to the pattern of change commonly described on the Tibetan Plateau and confirmed in this study in the northern Koshi Basin. However, this trend is in contrast with studies located south of the Himalayan ridge. As proved by this study, the southern Koshi Basin experienced a prevalence of maximum temperature increases. No linear pattern emerges in the elevation dependency of temperature trends. We only observed higher minimum temperature trends at higher altitudes.
- 3) The total annual precipitation has considerably decreased. The annual rate of decrease ~~at high elevation~~above 5000 m a.s.l. is similar to the one –at lower altitudes on the southern side of the Koshi Basin, but the drier conditions of this remote environment make the fractional loss relatively more consistent. The precipitation at high elevation during the monsoon period is currently half of what it was twenty years ago. These observations confirm the monsoon weakening observed by previous studies in India and even in the Himalayas since the early 1980s. As opposed to the northern side of the Koshi Basin that shows in this study certain stability, as positive or stationary trends have been

observed by previous studies on the TP and more specifically in northern central Himalaya.

- 4) There is a significantly lower probability of snowfall in the glaciers ablation zones, while the lower temperature of the upper glaciers zones have so far guaranteed a stationary condition.

In general, this study contributes to change the perspective on how the climatic driver (temperature vs. precipitation) led the glacier responses in the last twenty years. ~~to a change perspective related to the climatic driver (temperature vs. precipitation) led the glacier responses in the last twenty years.~~

Without demonstrating the causes that could have led to the climate change pattern observed at the PYRAMID, we simply note the recent literature on hypotheses that accord with our observations. ~~for the case study.~~

In conclusion, we have here observed that weather stations at low elevations are not able to suitably describe the climate changes occurring ~~at high altitudes~~ above 5000 m a.s.l. and thus correctly interpret the impact observed on the cryosphere. This consideration stresses the great importance of long-term ground measurements at high elevation.

Author contributions

G.T., Y.M. and E.V. designed research; F.S. performed research; F.S., N.G., S.T., G.V. and E.R. analyzed data; F.S., N.G., E.R. and G.T. wrote the paper. P.C., P.S., N.G. and G.A. data quality check.

Acknowledgements

This work was supported by the MIUR through Ev-K2-CNR/SHARE and CNR-DTA/NEXTDATA project within the framework of the Ev-K2-CNR and Nepal Academy of Science and Technology (NAST). Sudeep Thakuri is recipient of the IPCC Scholarship Award under the collaboration between the IPCC Scholarship Programme and the Prince Albert II of Monaco Foundation's Young Researchers Scholarships Initiative.

References

- Abebe, A., Solomatine, D., and Venneker, R.: Application of adaptive fuzzy rule based models for reconstruction of missing precipitation events, Hydrolog. Sci. J., 45, 425–436, doi:10.1080/02626660009492339, 2000.
- Abudu, S., Bawazir, A. S., and King, J. P.: Infilling missing daily evapotranspiration data using neural networks, J. Irrig. Drain. E-asce, 136, 317–325, doi:10.1061/(ASCE)IR.1943-4774.0000197, 2010.
- Amatya, L. K., Cuccillato, E., Haack, B., Shadie, P., Sattar, N., Bajracharya, B., Shrestha, B. Caroli, P., Panzeri, D., Basani, M., Schommer, B., Flury, B. Salerno, F.,

and Manfredi, E. C.: Improving communication for management of social-ecological systems in high mountain areas: Development of methodologies and tools – The HKKH Partnership Project, *Mt. Res. Dev.*, 30, 69-79, doi:10.1659/MRD-JOURNAL-D-09-00084.1, 2010.

Bajracharya B., Uddin, K., Chettri, N., Shrestha, B., and Siddiqui, S. A.: Understanding land cover change using a harmonized classification system in the Himalayas: A case study from Sagarmatha National Park, Nepal, *Mt. Res. Dev.*, 30, 143–156, doi: 10.1659/MRD-JOURNAL-D-09-00044.1, 2010.

Barros, A. P., Kim, G., Williams, E., and Nesbitt, S. W.: Probing orographic controls in the Himalayas during the monsoon using satellite imagery, *Nat. Hazards Earth Syst. Sci.* 4, 29–51, doi:10.5194/nhess-4-29-2004, 2004.

Benn, D. I., Bolch, T., Hands, K., Gulley, J., Luckman, A., Nicholson, L. I., Quincey, D., Thompson, S., Toumi, R., and Wiseman, S.: Response of debris-covered glaciers in the Mount Everest region to recent warming, and implications for outburst flood hazards, *Earth-Sci. Rev.*, 114, 156–174, doi:10.1016/j.earscirev.2012.03.008, 2012.

Bertolani L., Bollasina, M., and Tartari, G.: Recent biannual variability of meteorological features in the Eastern Highland Himalayas, *Geophys. Res. Lett.*, 27, 2185-2188, doi:10.1029/1999GL011198, 2000.

Bhutiyan, M. R., Kale, V. S., and Pawar, N. J.: Long-term trends in maximum, minimum and mean annual air temperatures across the Northwestern Himalaya during the twentieth century, *Climatic Change*, 85, 159–177, doi:10.1007/s10584-006-9196-1, 2007.

Bocchiola, D. and Diolaiuti, G.: Evidence of climate change within the Adamello Glacier of Italy, *Theor. Appl. Climatol.*, 100, 351–369, doi:10.1007/s00704-009-0186-x, 2010.

Bolch T., Buchroithner, M., Pieczonka, T., and Kunert, A.: Planimetric and volumetric glacier changes in the Khumbu Himal, Nepal, since 1962 using Corona, Landsat TM and ASTER data, *J. Glaciol.*, 54, 592–600, doi: 0.3189/002214308786570782, 2008.

Bolch T., Kulkarni, A., Käab, A., Huggel, C., Paul, F., Cogley, J. G., Frey, H., Kargel, J. S., Fujita, K., Scheel, M., Bajracharya, S., and Stoffel, M.: The state and fate of Himalayan glaciers, *Science*, 336, 310-314, doi: 10.1126/science.1215828, 2012.

Bolch T., Pieczonka, T., and Benn, D.I.: Multi-decadal mass loss of glaciers in the Everest area (Nepal Himalaya) derived from stereo imagery, *The Cryosphere*, 5, 349–358, doi:10.5194/tc-5-349-2011, 2011.

Bollasina, M. A., Ming, Y., and Ramaswamy, V.: Anthropogenic aerosols and the weakening of the south Asian summer monsoon, *Science*, 334, 502-505, doi:10.1126/science.1204994, 2011.

Bookhagen, B. and Burbank, D. W.: Topography, relief, and TRMM-derived rainfall variations along the Himalaya, *Geophys. Res. Lett.*, 33, L08405, doi:10.1029/2006GL026037, 2006.

Carraro, E., Guyennon, N., Hamilton, D., Valsecchi, L., Manfredi, E. C., Viviano, G., Salerno, F., Tartari, G., and Copetti, D.: Coupling high-resolution measurements to a

three-dimensional lake model to assess the spatial and temporal dynamics of the cyanobacterium *Planktothrix rubescens* in a medium-sized lake, *Hydrobiologia*, 698 (1), 77-95. doi:10.1007/s10750-012-1096-y, 2012.

Carraro, E., Guyennon, N., Viviano, G., Manfredi, E. C., Valsecchi, L., Salerno, F., Tartari, G., and Copetti, D.: Impact of Global and Local Pressures on the Ecology of a Medium-Sized Pre-Alpine Lake, in *Models of the Ecological Hierarchy*, edited by: Jordan, F., and Jorgensen, S. E., Elsevier B.V., pp. 259-274, doi:10.1016/B978-0-444-59396-2.00016-X, 2012b.

Coulilaly, P. and Evora, N.: Comparison of neural network methods for infilling missing daily weather records, *J. Hydrol.*, 341, 27–41, doi:10.1016/j.jhydrol.2007.04.020, 2007.

Déqué, M.: Frequency of precipitation and temperature extremes over France in an anthropogenic scenario: model results and statistical correction according to observed values, *Global Planet. Change*, 57, 16–26, doi:10.1016/j.gloplacha.2006.11.030, 2007.

Duan, A. and Wu, G.: Change of cloud amount and the climate warming on the Tibetan Plateau, *Geophys. Res. Lett.*, 33, L22704, doi:10.1029/2006GL027946, 2006.

Dytham, C.: *Choosing and Using Statistics: A Biologist's Guide*, John Wiley & Sons, 2011.

Fujita, K., and Sakai, A.: Modelling runoff from a Himalayan debris-covered glacier, *Hydrol. Earth Syst. Sci.*, 18, 2679–2694, doi:10.5194/hess-18-2679-2014, 2014.

Fujita, K., Sakai, A., Takenaka, S., Nuimura, T., Surazakov, A. B., Sawagaki, T., and Yamanokuchi T.: Potential flood volume of Himalayan glacial lakes, *Nat. Hazards Earth Syst. Sci.*, 13, 1827–1839, doi:10.5194/nhessd-1-15-2013, 2013.

Ganguly, N. D. and Iyer, K. N.: Long-term variations of surface air temperature during summer in India, *Int. J. Climatol.*, 29, 735–746, doi:10.1002/joc.1748, 2009.

Gardelle, J., Arnaud, Y., and Berthier, E.: Contrasted evolution of glacial lakes along the Hindu Kush Himalaya mountain range between 1990 and 2009, *Global Planet. Change*, 75, 47-55, doi:10.1016/j.gloplacha.2010.10.003, 2011.

Gautam, R., Hsu, N. C. and Lau, K. M.: Premonsoon aerosol characterization and radiative effects over the Indo-Gangetic plains: implications for regional climate warming, *J. Geophys. Res.*, 115, D17208, doi:10.1029/2010JD013819, 2010.

Gerstengarbe, F. W. and Werner, P. C.: Estimation of the beginning and end of recurrent events within a climate regime, *Clim. Res.*, 11, 97-107, 1999.

Guyennon, N., Romano, E., Portoghesi, I., Salerno, F., Calmanti, S., Petrangeli, A. B., Tartari, G., and Copetti, D.: Benefits from using combined dynamical-statistical downscaling approaches – lessons from a case study in the Mediterranean region, *Hydrol. Earth Syst. Sc.*, 17, 705–720, doi:10.5194/hess-17-705-2013, 2013.

Hock, R.: Glacier melt: a review of processes and their modeling, *Prog. Phys. Geog.*, 29, 362-391, doi:10.1191/0309133305pp453ra, 2005.

Ichiyanagi, K., Yamanaka, M. D., Muraji, Y., and Vaidya, B. K.: Precipitation in Nepal between 1987 and 1996, *Int. J. Climatol.*, 27, 1753–1762, doi:10.1002/joc.1492,

2007.

Immerzeel, W. W., Petersen, L., Ragettli, S., and Pellicciotti, F.: The importance of observed gradients of air temperature and precipitation for modeling runoff from a glacierized watershed in the Nepal Himalayas, *Water Resour. Res.*, 50, doi:10.1002/2013WR014506, 2014.

James, A. L. and Oldenburg, C. M.: Linear and Monte Carlo uncertainty analysis for subsurface contaminant transport simulation, *Water Resour. Res.*, 33, 2495–2508, doi:10.1029/97WR01925, 1997.

Kattel, D. B. and Yao, T.: Recent temperature trends at mountain stations on the southern slope of the central Himalayas, *J. Earth Syst. Sci.*, 122, 215–227, doi:10.1007/s12040-012-0257-8, 2013.

Kendall, M.G.: *Rank Correlation Methods*, Oxford University Press, New York, 1975.

Kivekas, N., Sun, J., Zhan, M., Kerminen, V. M., Hyvarinen, A., Komppula, M., Viisanen, Y., Hong, N., Zhang, Y., Kulmala, M., Zhang, X. C., Deli-Geer, and Lihavainen, H.: Long term particle size distribution measurements at Mount Waliguan, a high-altitude site in inland China, *Atmos. Chem. Phys.*, 9, 5461–5474, doi:10.5194/acp-9-95461-2009, 2009.

Lami, A., Marchetto, A., Musazzi, S., Salerno, F., Tartari, G., Guilizzoni, P., Rogora, M., and Tartari, G. A.: Chemical and biological response of two small lakes in the Khumbu Valley, Himalayas (Nepal) to short-term variability and climatic change as detected by long-term monitoring and paleolimnological methods, *Hydrobiologia*, 648, 189–205, doi:10.1007/s10750-010-0262-3, 2010.

Lau, K.-M., and Kim, K.-M.: Observational relationships between aerosol and Asian monsoon rainfall, and circulation, *Geophys. Res. Lett.*, 33, L21810, doi:10.1029/2006GL027546, 2006.

Lavagnini, I., Badocco, D., Pastore, P., and Magno, F.: Theil-Sen nonparametric regression technique on univariate calibration, inverse regression and detection limits, *Talanta*, 87, 180–188, doi:10.1016/j.talanta.2011.09.059, 2011.

Levy II, H., L. W., Horowitz, M. D., Schwarzkopf, Y., Ming, J. C., Golaz, V., Naik, and Ramaswamy, V.: The roles of aerosol direct and indirect effects in past and future climate change, *J. Geophys. Res.*, 118, 1–12, doi:10.1002/jgrd.50192, 2013.

Liu, J., Yang, B., and Qin, C.: Tree-ring based annual precipitation reconstruction since AD 1480 in south central Tibet. *Quatern. Int.*, 236, 75–81, doi:10.1016/j.quaint.2010.03.020, 2010.

Liu, K., Cheng, Z., Yan, L., and Yin, Z.: Elevation dependency of recent and future minimum surface air temperature trends in the Tibetan Plateau and its surroundings, *Global Planet. Change*, 68, 164–174, doi:10.1016/j.gloplacha.2009.03.017, 2009.

Liu, X. D., and Chen, B. D.: Climatic warming in the Tibetan Plateau during recent decades, *Int. J. Climatol.*, 20, 1729–1742, doi:10.1002/1097-0088(20001130)20:14<1729::AID-JOC556>3.0.CO;2-Y, 2000.

Liu, X.D., Yin, Z. Y., Shao, X., and Qin, N.: Temporal trends and variability of daily maximum and minimum, extreme temperature events, and growing season length

over the eastern and central Tibetan Plateau during 1961–2003, *J. Geophys. Res.*, 111, D19, doi:10.1029/2005JD006915, 2006.

Manfredi, E. C., Flury, B., Viviano, G., Thakuri, S., Khanal, S. N., Jha, P. K., Maskey, R. K., Kayastha, R. B., Kafle, K. R., Bhochhibhoya, S., Ghimire, N. P., Shrestha, B. B., Chaudhary, G., Giannino, F., Carteni, F., Mazzoleni, S., and Salerno, F.: Solid waste and water quality management models for Sagarmatha National Park and Buffer Zone, Nepal: implementation of a participatory modeling framework, *Mt. Res. Dev.*, 30, 127–142, doi:10.1659/MRD-JOURNAL-D-10-00028.1, 2010.

Marinoni, A., Cristofanelli, P., Laj, P., Putero, D., Calzolari, F., Landi, T. C., Vuillermoz, E., Maione, M., and Bonasoni, P.: High black carbon and ozone concentrations during pollution transport in the Himalayas: Five years of continuous observations at NCO-Prec global GAW station, *J. Environ. Sci.*, 25, 1618–1625, doi:10.1016/S1001-0742(12)60242-3, 2013.

Menne, M. J., Durre, I., Vose, R. S., Gleason, B. E., and Houston, T. G.: An overview of the Global Historical Climatology Network—daily database, *J. Atmos. Oceanic Technol.*, 29, 897–910, 2012.

Mitchell, J. F. B. and Johns, T. C.: On the modification of global warming by sulphate aerosols, *J. Climate*, 10, 245–267, 1997.

Montgomery, D. R. and Stolar, D. B.: Reconsidering Himalayan river anticlines, *Geomorphology*, 82, 4–15, doi:10.1016/j.geomorph.2005.08.021, 2006.

Moss, R. H., et al.: The next generation of scenarios for climate change research and assessment, *Nature*, 463, 747–756, doi:10.1038/nature08823, 2010.

Nuimura, T., Fujita, K., Yamaguchi, S., and Sharma, R. R.: Elevation changes of glaciers revealed by multitemporal digital elevation models calibrated by GPS survey in the Khumbu region, Nepal Himalaya, 1992–2008, *J. Glaciol.*, 58, 648–656, doi:10.3189/2012JoG11J061, 2012.

Pal, I. and Al-Tabbaa, A.: Long-term changes and variability of monthly extreme temperatures in India, *Theor. Appl. Climatol.*, 100, 45–56, doi:10.1007/s00704-009-0167-0, 2010.

Palazzi, E., von Hardenberg, J., and Provenzale, A.: Precipitation in the Hindu-Kush Karakoram Himalaya: Observations and future scenarios, *J. Geophys. Res.*, 118, 85–100, doi: 10.1029/2012JD018697, 2013.

Pepin, N. C. and Lundquist, J. D.: Temperature trends at high elevations: patterns across the globe, *Geophys. Res. Lett.*, 35, doi:10.1029/2008GL034026, 2008.

Peters, J., Bolch, T., Buchroithner, M. F., and Bäßler, M.: Glacier Surface Velocities in the Mount Everest Area/Nepal using ASTER and Ikonos imagery, *Proceeding of 10th International Symposium on High Mountain Remote Sensing Cartography, Kathmandu, Nepal*, 313–320, 2010.

Putero, D., T. C., Landi, P., Cristofanelli, A., Marinoni, P., Laj, R., Duchi, F., Calzolari, G. P., Verza and P. Bonasoni, Influence of open vegetation fires on black carbon and ozone variability in the southern Himalayas (NCO-P, 5079 m a.s.l.), *Environ. Pollut.*, 184, 597–604, doi: 10.1016/j.envpol.2013.09.035, 2013.

Qian, Y., Flanner, M., Leung, L., and Wang, W.: Sensitivity studies on the impacts of Tibetan plateau snowpack pollution on the Asian hydrological cycle and monsoon climate, *Atmos. Chem. Phys.*, 11, 1929–1948, doi:10.5194/acp-11-1929-2011, 2011.

Quincey, D. J., Luckman, A., and Benn, D.: Quantification of Everest region glacier velocities between 1992 and 2002, using satellite radar interferometry and feature tracking, *J. Glaciol.*, 55, 596–606, doi: 10.3189/002214309789470987, 2009.

Ramanathan, V., Chung, C., Kim, D., Bettge, T., Buja, L., Kiehl, J. T., Washington, W. M., Fu, Q., Sikka, D. R., and Wild, M.: Atmospheric brown clouds: Impacts on South Asian climate and hydrological cycle. *Proc. Natl. Acad. Sci. U.S.A.*, 102, 5326– 5333, doi: 10.1073/pnas.0500656102, 2005.

Ramanathan, V., Li, F., Ramana, M. V., Praveen, P. S., Kim, D., Corrigan, C. E., Nguyen, H., Stone, E. A., Schauer, J. J., Carmichael, G. R., Adhikary, B., and Yoon, S. C.: Atmospheric brown clouds: Hemispherical and regional variations in long-range transport, absorption, and radiative forcing, *J. Geophys. Res.*, 112, D22, doi:10.1029/2006JD008124, 2007.

Rangwala, I. and Miller, J. R.: Climate change in mountains: a review of elevation-dependent warming and its possible causes, *Climatic Change*, 114, 527–547, doi:10.1007/s10584-012-0419-3, 2012.

Rangwala, I., Barsugli, J., Cozzetto, K., Neff, J., and Prairie, J.: Mid-21st century projections in temperature extremes in the southern Colorado Rocky Mountains from regional climate models, *Clim Dyn.*, 39, 1823–1840, doi:10.1007/s00382- 011-1282-z, 2012.

Rikiishi, K. and Nakasato, H.: Height dependence of the tendency for reduction in seasonal snow cover in the Himalaya and the Tibetan Plateau region, 1966–2001, *Ann. Glaciol.*, 43, 369–377, doi: http://dx.doi.org/10.3189/172756406781811989, 2006.

Salerno, F., Buraschi, E., Bruccoleri, G., Tartari, G., and Smiraglia, C.: Glacier surface-area changes in Sagarmatha National Park, Nepal, in the second half of the 20th century, by comparison of historical maps, *J. Glaciol.*, 54, 738–752, 2008.

Salerno, F., Cuccillato, E., Caroli, P., Bajracharya, B., Manfredi, E. C., Viviano, G., Thakuri, S., Flury, B., Basani, M., Giannino, F., and Panzeri, D.: Experience with a hard and soft participatory modeling framework for social ecological system management in Mount Everest (Nepal) and K2 (Pakistan) protected areas, *Mt. Res. Dev.*, 30, 80–93, 2010a.

Salerno, F., Gambelli, S., Viviano, G., Thakuri, S., Guyennon, N., D’Agata, C., Diolaiuti, G., Smiraglia, C., Stefani, F., Bochiola, D., and Tartari, G.: High alpine ponds shift upwards as average temperature increase: A case study of the Ortles-Cevedale mountain group (Southern alps, Italy) over the last 50 years, *Global Planet. Change*, doi: 10.1016/j.gloplacha.2014.06.003, 2014.

Salerno, F., Thakuri, S., D’Agata, C., Smiraglia, C., Manfredi, E. C., Viviano, G., and Tartari, G.: Glacial lake distribution in the Mount Everest region: Uncertainty of measurement and conditions of formation, *Global Planet. Change*, 92–93, 30–39,

doi:10.1016/j.gloplacha.2012.04.001, 2012.

Salerno, F., Viviano, G., Mangredi, E. C., Caroli, P., Thakuri, S., and Tartari, G.: Multiple Carrying Capacities from a management-oriented perspective to operationalize sustainable tourism in protected area, *J. Environ. Manage.*, 128, 116-125, doi:10.1016/j.jenvman.2013.04.043, 2013.

Salerno, F., Viviano, G., Thakuri, S., Flury, B., Maskey, R. K., Khanal, S. N., Bhuju, D., Carrer, M., Bhochhibhoya, S., Melis, M. T., Giannino, F., Staiano, A., Carteni, F., Mazzoleni, S., Cogo, A., Sapkota, A., Shrestha, S., Pandey, R. K., and Manfredi, E. C.: Energy, forest, and indoor air pollution models for Sagarmatha National Park and Buffer zone, Nepal: implementation of a participatory modeling framework, *Mt. Res. Dev.*, 30, 113–126, 2010b.

Scherler, D., Bookhagen, B., and Strecker, M. R.: Spatially variable response of Himalayan glaciers to climate change affected by debris cover, *Nature Geosci.*, 4, 156–159, doi:10.1038/ngeo1068, 2011.

Schneider, T.: Analysis of incomplete climate data: Estimation of mean values and covariance matrices and imputation of missing values, *J. Clim.*, 14, 853–871, doi:10.1175/1520-0442(2001)014<0853:AOICDE>2.0.CO;2, 2001.

Sellegrì, K., Laj, P., Venzac, H., Boulon, J., Picard, D., Villani, P., Bonasoni, P., Marinoni, A., Cristofanelli, P., and Vuillermoz, E.: Seasonal variations of aerosol size distributions based on long-term measurements at the high altitude Himalayan site of Nepal Climate Observatory—Pyramid (5079 m), Nepal, *Atmos. Chem. Phys.*, 10, 10679–10690, doi:10.5194/acp-10.10679-2010, 2010.

Sen, P. K.: Estimates of the regression coefficient based on Kendall's Tau, *J. Am. Assoc.*, 63, 1379-1389, doi:10.2307/2285891, 1968.

Shekhar, M. S., Chand, H., Kumar, S., Srinivasan, K., and Ganju, A.: Climate-change studies in the western Himalaya, *Ann. Glaciol.*, 51, 105-112, doi:10.3189/172756410791386508, 2010.

Shrestha, A. B., Wake, C. P., Mayewski, P. A., and Dibb, J. E.: Maximum temperature trends in the Himalaya and its vicinity: An analysis based on temperature records from Nepal for the period 1971-94, *J. Clim.*, 12, 2775-5561, doi:10.1175/1520-0442(1999)012<2775:MTTITH>2.0.CO;2, 1999.

Singh, P. and Kumar, N.: Effect of orography on precipitation in the western Himalayan region, *J. Hydrol.*, 199, 183-206, doi:10.1016/S0022-1694(96)03222-2, 1997.

Su, B. D., Jiang, T., and Jin, W. B.: Recent trends in observed temperature and precipitation extremes in the Yangtze River basin, China, *Theor. Appl. Climatol.*, 83, 139–151, doi:10.1007/s00704-005-0139-y, 2006.

Tartari, G., Salerno, F., Buraschi, E., Bruccoli, G., and Smiraglia, C.: Lake surface area variations in the North-Eastern sector of Sagarmatha National Park (Nepal) at the end of the 20th Century by comparison of historical maps, *J. Limnol.*, 67, 139-154, doi:10.4081/jlimnol.2008.139, 2008.

Tartari, G., Verza, P., and Bertolami, L.: Meteorological data at PYRAMID Observatory Laboratory (Khumbu Valley, Sagarmatha National Park, Nepal), in *Limnology of*

high altitude lakes in the Mt. Everest Region (Nepal), edited by: Lami, A. and Giussani, G., *Mem. Ist. Ital. Idrobiol*, 57, 23-40, 2002.

Tartari, G., Vuillermoz, E., Manfredi, E. C., and Toffolon, R.: CEOP High Elevations Initiative, *GEWEX News, Special Issue*, 19(3), 4-5, 2009.

Thakuri, S., Salerno, F., Smiraglia, C., Bolch, T., D'Agata, C., Viviano, G., and Tartari, G.: Tracing glacier changes since the 1960s on the south slope of Mt. Everest (central southern Himalaya) using optical satellite imagery, *The Cryosphere*, 8, 1297-1315, doi:10.5194/tc-8-1297-2014, 2014.

Thiemeßl, M. J., Gobiet, A., and Heinrich, G.: Empirical-statistical downscaling and error correction of regional climate models and its impact on the climate change signal, *Climatic Change*, 112, 449-468, doi:10.1007/s10584-011-011-0224-4, 2012.

Turner, A. G. and Annamalai, H.: Climate change and the South Asian summer monsoon, *Nat. Clim. Change*, 2, 587-595, doi:10.1038/nclimate1495, 2012.

Ueno K. and Aryal, R.: Impact of tropical convective activity on monthly temperature variability during non monsoon season in the Nepal Himalayas, *J. Geophys. Res.*, 113, D18112, doi:10.1029/2007JD009524, 2008.

Ueno, K., Endoh, N., Ohata, T., Yabuki, H., Koike, M., and Zhang, Y.: Characteristics of precipitation distribution in Tangua, Monsoon, 1993, *Bulletin of Glaciological Research*, 12, 39-46, 1994.

UNEP (United Nations Environment Programme)/WCMC (World Conservation Monitoring Centre): Sagarmatha National Park, Nepal, in *Encyclopedia of Earth*, edited by: McGinley, M. and Cleveland, C. J., Environmental Information Coalition, National Council for Science and the Environment, Washington, DC, 2008.

Venzac, H., Sellegri, K., Laj, P., Villani, P., Bonasoni, P., Marinoni, A., Cristofanelli, P., Calzolari, F., Fuzzi, S., Decesari, S., Facchini, M. C., Vuillermoz, E., and Verza, G. P.: High frequency new particle formation in the Himalayas, *Proc. Natl. Acad. Sci. USA*, 105, 15666-15671, doi:10.1073/pnas.0801355105, 2008.

Vuille, M.: Climate variability and high altitude temperature and precipitation, in *Encyclopedia of snow, ice and glaciers*, edited by: Singh, V. P. et al., Springer, pp. 153-156, 2011.

Wagnon, P., Vincent, C., Arnaud, Y., Berthier, E., Vuillermoz, E., Gruber, S., Ménégoz, M., Gilbert, A., Dumont, M., Shea, J. M., Stumm, D., and Pokhrel, B. P.: Seasonal and annual mass balances of Mera and Pokalde glaciers (Nepal Himalaya) since 2007, *The Cryosphere*, 7, 1769-1786, doi:10.5194/tc-7-1769-2013, 2013.

Washington, W. M. and Parkinson, C. L.: An introduction to three-Dimensional Climate Modeling, 2nd Edition, University Science Books, Sausalito, 2005.

Wu, B.: Weakening of Indian summer monsoon in recent decades, *Adv. Atmos. Sci.*, 22(1), 21-29, doi:10.1007/BF02930866, 2005.

Yang J., Tan, C., and Zhang, T.: Spatial and temporal variations in air temperature and precipitation in the Chinese Himalayas during the 1971–2007, *Int. J. Climatol.*, 33, 2622-2632, doi:10.1002/joc.3609, 2012.

Yang, X., Zhang, Y., Zhang, W., Yan, Y., Wang, Z., Ding, M., and Chu, D.: Climate

change in Mt. Qomolangma region since 1971, *J. Geogr. Sci.*, 16, 326-336, doi:10.1007/s11442-006-0308-7, 2006.

Yao, T., Thompson, L., Yang, W., Yu, W., Gao, Y., Guo, X., Yang, X., Duan, K., Zhao, H., Xu, B., Pu, J., Lu, A., Xiang, Y., Kattel, D. B., and Joswiak, D.: Different glacier status with atmospheric circulations in Tibetan Plateau and surroundings, *Nat. Clim. Change*, 2, 663-667, doi:10.1038/nclimate1580, 2012.

Yasutomi, N., Hamada, A., and Yatagai, A.: Development of a long-term daily gridded temperature dataset and its application to rain/snow discrimination of daily precipitation, *Global Environ. Res.*, V15N2, 165-172, 2011.

You, Q., Kang, S., Pepin, N., Flügel, W., Yan, Y., Behrawan, H., and Huang, J.: Relationship between temperature trend magnitude, elevation and mean temperature in the Tibetan Plateau from homogenized surface stations and reanalysis data, *Global Planet. Change*, 71, 124-133, doi:10.1016/j.gloplacha.2010.01.020, 2010.

Zhao, H., Xu, B., Yao, T., Wu, G., Lin, S., Gao, J., and Wang, M.: Deuterium excess record in a southern Tibetan ice core and its potential climatic implications, *Clim. Dyn.*, 38, 1791-1803, doi:10.1007/s00382-011-1161-7, 2012.

~~Fujita, K., and Sakai, A.: Modelling runoff from a Himalayan debris-covered glacier, *Hydrol. Earth Syst. Sci.*, 18, 2679–2694, doi:10.5194/hess-18-2679-2014, 2014.~~

~~Ueno, K., Endoh, N., Ohata, T., Yabuki, H., Koike, M., and Zhang, Y.: Characteristics of precipitation distribution in Tangua, Monsoon, 1993, *Bulletin of Glaciological Research*, 12, 39–46, 1994.~~

~~Abebe, A., Solomatine, D., and Venneker, R.: Application of adaptive fuzzy rule based models for reconstruction of missing precipitation events, *Hydrolog. Sci. J.*, 45, 425–436, doi:10.1080/02626660009492339, 2000.~~

~~Abudu, S., Bawazir, A. S., and King, J. P.: Infilling missing daily evapotranspiration data using neural networks, *J. Irrig. Drain. E-asc*, 136, 317–325, doi:10.1061/(ASCE)IR.1943-4774.0000197, 2010.~~

~~Amatya, L. K., Cuccillato, E., Haack, B., Shadie, P., Sattar, N., Bajracharya, B., Shrestha, B., Caroli, P., Panzeri, D., Basani, M., Schommer, B., Flury, B., Salerno, F., and Manfredi, E. C.: Improving communication for management of social-ecological systems in high mountain areas: Development of methodologies and tools—The HKKH Partnership Project, *Mt. Res. Dev.*, 30, 69–79, doi:10.1659/MRD-JOURNAL-D-09-00084.1, 2010.~~

~~Bajracharya B., Uddin, K., Chettri, N., Shrestha, B., and Siddiqui, S. A.: Understanding land cover change using a harmonized classification system in the Himalayas: A case study from Sagarmatha National Park, Nepal, *Mt. Res. Dev.*, 30, 143–156, doi:10.1659/MRD-JOURNAL-D-09-00044.1, 2010.~~

~~Barros, A. P., Kim, G., Williams, E., and Nesbitt, S. W.: Probing orographic controls in the Himalayas during the monsoon using satellite imagery, *Nat. Hazards Earth Syst. Sci.*, 4, 29–51, doi:10.5194/nhess-4-29-2004, 2004.~~

~~Benn, D. I., Bolch, T., Hands, K., Gulley, J., Luckman, A., Nicholson, L. I., Quincey,~~

~~D., Thompson, S., Toumi, R., and Wiseman, S.: Response of debris-covered glaciers in the Mount Everest region to recent warming, and implications for outburst flood hazards, *Earth Sci. Rev.*, 114, 156–174, doi:10.1016/j.earseirev.2012.03.008, 2012.~~

~~Bertolani L., Bollasina, M., and Tartari, G.: Recent biannual variability of meteorological features in the Eastern Highland Himalayas, *Geophys. Res. Lett.*, 27, 2185–2188, doi:10.1029/1999GL011198, 2000.~~

~~Bhutiyani, M. R., Kale, V. S., and Pawar, N. J.: Long-term trends in maximum, minimum and mean annual air temperatures across the Northwestern Himalaya during the twentieth century, *Climatic Change*, 85, 159–177, doi:10.1007/s10584-006-9196-1, 2007.~~

~~Bocchiola, D. and Diolaiuti, G.: Evidence of climate change within the Adamello Glacier of Italy, *Theor. Appl. Climatol.*, 100, 351–369, doi:10.1007/s00704-009-0186-x, 2010.~~

~~Bolch T., Kulkarni, A., Kääb, A., Huggel, C., Paul, F., Cogley, J. G., Frey, H., Kargel, J. S., Fujita, K., Scheel, M., Bajracharya, S., and Stoffel, M.: The state and fate of Himalayan glaciers, *Science*, 336, 310–314, doi: 10.1126/science.1215828, 2012.~~

~~Bolch T., Buchroithner, M., Pieczonka, T., and Kunert, A.: Planimetric and volumetric glacier changes in the Khumbu Himal, Nepal, since 1962 using Corona, Landsat TM and ASTER data, *J. Glaciol.*, 54, 592–600, doi: 0.3189/002214308786570782, 2008.~~

~~Bolch T., Pieczonka, T., and Benn, D.I.: Multi-decadal mass loss of glaciers in the Everest area (Nepal Himalaya) derived from stereo imagery, *The Cryosphere*, 5, 349–358, doi:10.5194/tc-5-349-2011, 2011.~~

~~Bollasina, M. A., Ming, Y., and Ramaswamy, V.: Anthropogenic aerosols and the weakening of the south Asian summer monsoon, *Science*, 334, 502–505, doi:10.1126/science.1204994, 2011.~~

~~Bookhagen, B. and Burbank, D. W.: Topography, relief, and TRMM-derived rainfall variations along the Himalaya, *Geophys. Res. Lett.*, 33, L08405, doi:10.1029/2006GL026037, 2006.~~

~~Carraro, E., Guyennon, N., Hamilton, D., Valsecchi, L., Manfredi, E. C., Viviano, G., Salerno, F., Tartari, G., and Copetti, D.: Coupling high-resolution measurements to a three-dimensional lake model to assess the spatial and temporal dynamics of the cyanobacterium *Planktothrix rubescens* in a medium-sized lake, *Hydrobiologia*, 698 (1), 77–95. doi:10.1007/s10750-012-1096-y, 2012.~~

~~Carraro, E., Guyennon, N., Viviano, G., Manfredi, E. C., Valsecchi, L., Salerno, F., Tartari, G., and Copetti, D.: Impact of Global and Local Pressures on the Ecology of a Medium-Sized Pre-Alpine Lake, in *Models of the Ecological Hierarchy*, edited by: Jordan, F., and Jorgensen, S. E., Elsevier B.V., pp. 259–274, doi:10.1016/B978-0-444-59396-2.00016-X, 2012b.~~

~~Coulibaly, P. and Evora, N.: Comparison of neural network methods for infilling missing daily weather records, *J. Hydrol.*, 341, 27–41, doi:10.1016/j.jhydrol.2007.04.020, 2007.~~

~~Déqué, M.: Frequency of precipitation and temperature extremes over France in an~~

anthropogenic scenario: model results and statistical correction according to observed values, *Global Planet. Change*, 57, 16–26, doi:10.1016/j.gloplacha.2006.11.030, 2007.

Duan, A. and Wu, G.: Change of cloud amount and the climate warming on the Tibetan Plateau, *Geophys. Res. Lett.*, 33, L22704, doi:10.1029/2006GL027946, 2006.

Dytham, C.: *Choosing and Using Statistics: A Biologist's Guide*, John Wiley & Sons, 2011.

Fujita, K., Sakai, A., Takenaka, S., Nuimura, T., Surazakov, A. B., Sawagaki, T., and Yamanokuchi T.: Potential flood volume of Himalayan glacial lakes, *Nat. Hazards Earth Syst. Sci.*, 13, 1827–1839, doi:10.5194/nhessd-1-15-2013, 2013.

Ganguly, N. D. and Iyer, K. N.: Long term variations of surface air temperature during summer in India, *Int. J. Climatol.*, 29, 735–746, doi:10.1002/joc.1748, 2009.

Gardelle, J., Arnaud, Y., and Berthier, E.: Contrasted evolution of glacial lakes along the Hindu Kush Himalaya mountain range between 1990 and 2009, *Global Planet. Change*, 75, 47–55, doi:10.1016/j.gloplacha.2010.10.003, 2011.

Gautam, R., Hsu, N. C. and Lau, K. M.: Premonsoon aerosol characterization and radiative effects over the Indo Gangetic plains: implications for regional climate warming, *J. Geophys. Res.*, 115, D17208, doi:10.1029/2010JD013819, 2010.

Gerstengarbe, F. W. and Werner, P. C.: Estimation of the beginning and end of recurrent events within a climate regime, *Clim. Res.*, 11, 97–107, 1999.

Guyennon, N., Romano, E., Portoghesi, I., Salerno, F., Calmanti, S., Petrangeli, A. B., Tartari, G., and Copetti, D.: Benefits from using combined dynamical statistical downscaling approaches—lessons from a case study in the Mediterranean region, *Hydrol. Earth Syst. Sc.*, 17, 705–720, doi:10.5194/hess-17-705-2013, 2013.

Hoek, R.: Glacier melt: a review of processes and their modeling, *Prog. Phys. Geog.*, 29, 362–391, doi:10.1191/0309133305pp453ra, 2005.

Ichiyanagi, K., Yamanaka, M. D., Muraji, Y., and Vaidya, B. K.: Precipitation in Nepal between 1987 and 1996, *Int. J. Climatol.*, 27, 1753–1762, doi:10.1002/joc.1492, 2007.

Immerzeel, W. W., Petersen, L., Ragettli, S., and Pellicciotti, F.: The importance of observed gradients of air temperature and precipitation for modeling runoff from a glacierized watershed in the Nepal Himalayas, *Water Resour. Res.*, 50, doi:10.1002/2013WR014506, 2014.

James, A. L. and Oldenburg, C. M.: Linear and Monte Carlo uncertainty analysis for subsurface contaminant transport simulation, *Water Resour. Res.*, 33, 2495–2508, doi:10.1029/97WR01925, 1997.

Kattel, D. B. and Yao, T.: Recent temperature trends at mountain stations on the southern slope of the central Himalayas, *J. Earth Syst. Sci.*, 122, 215–227, doi:10.1007/s12040-012-0257-8, 2013.

Kendall, M. G.: *Rank Correlation Methods*, Oxford University Press, New York, 1975.

Kivekas, N., Sun, J., Zhan, M., Kerminen, V. M., Hyvarinen, A., Komppula, M., Viisanen, Y., Hong, N., Zhang, Y., Kulmala, M., Zhang, X. C., Deli-Geer, and

~~Lihavainen, H.: Long term particle size distribution measurements at Mount~~
~~Waliguan, a high altitude site in inland China, Atmos. Chem. Phys., 9, 5461–5474,~~
~~doi:10.5194/acp-9-95461-2009, 2009.~~
~~Lami, A., Marchetto, A., Musazzi, S., Salerno, F., Tartari, G., Guilizzoni, P., Rogora, M.,~~
~~and Tartari, G. A.: Chemical and biological response of two small lakes in the~~
~~Khumbu Valley, Himalayas (Nepal) to short term variability and climatic change as~~
~~detected by long term monitoring and paleolimnological methods, Hydrobiologia,~~
~~648, 189–205, doi:10.1007/s10750-010-0262-3, 2010.~~
~~Lau, K. M., and Kim, K. M.: Observational relationships between aerosol and Asian~~
~~monsoon rainfall, and circulation, Geophys. Res. Lett., 33, L21810,~~
~~doi: 10.1029/2006GL027546, 2006.~~
~~Lavagnini, I., Badoeco, D., Pastore, P., and Magno, F.: Theil–Sen nonparametric regres-~~
~~sion technique on univariate calibration, inverse regression and detection limits, Ta-~~
~~lanta, 87, 180–188, doi:10.1016/j.talanta.2011.09.059, 2011.~~
~~Levy H, H., L. W., Horowitz, M. D., Schwarzkopf, Y., Ming, J. C., Golaz, V., Naik, and~~
~~Ramaswamy, V.: The roles of aerosol direct and indirect effects in past and future~~
~~climate change, J. Geophys. Res., 118, 1–12, doi:10.1002/jgrd.50192, 2013.~~
~~Liu, J., Yang, B., and Qin, C.: Tree-ring based annual precipitation reconstruction since~~
~~AD 1480 in south central Tibet. Quatern. Int., 236, 75–81,~~
~~doi:10.1016/j.quaint.2010.03.020, 2010.~~
~~Liu, K., Cheng, Z., Yan, L., and Yin, Z.: Elevation dependency of recent and future min-~~
~~imum surface air temperature trends in the Tibetan Plateau and its surroundings,~~
~~Global Planet. Change, 68, 164–174, doi:10.1016/j.gloplacha.2009.03.017, 2009.~~
~~Liu, X. D., and Chen, B. D.: Climatic warming in the Tibetan Plateau during recent~~
~~decades, Int. J. Climatol., 20, 1729–1742, doi:10.1002/1097-~~
~~0088(20001130)20:14<1729::AID-JOC556>3.0.CO;2-Y, 2000.~~
~~Liu, X.D., Yin, Z. Y., Shao, X., and Qin, N.: Temporal trends and variability of daily~~
~~maximum and minimum, extreme temperature events, and growing season length~~
~~over the eastern and central Tibetan Plateau during 1961–2003, J. Geophys. Res.,~~
~~111, D19, doi:10.1029/2005JD006915, 2006.~~
~~Manfredi, E. C., Flury, B., Viviano, G., Thakuri, S., Khanal, S. N., Jha, P. K., Maskey,~~
~~R. K., Kayastha, R. B., Kafle, K. R., Bhochhibhoya, S., Ghimire, N. P., Shrestha, B.~~
~~B., Chaudhary, G., Giannino, F., Carteni, F., Mazzoleni, S., and Salerno, F.: Solid~~
~~waste and water quality management models for Sagarmatha National Park and~~
~~Buffer Zone, Nepal: implementation of a participatory modeling framework, Mt.~~
~~Res. Dev., 30, 127–142, doi:10.1659/MRD-JOURNAL-D-10-00028.1, 2010.~~
~~Marinoni, A., Cristofanelli, P., Laj, P., Putero, D., Calzolari, F., Landi, T. C., Vuillermoz,~~
~~E., Maione, M., and Bonasoni, P.: High black carbon and ozone concentrations~~
~~during pollution transport in the Himalayas: Five years of continuous observations at~~
~~NCO-Prec global GAW station, J. Environ. Sci., 25, 1618–1625, doi:10.1016/S1001-~~
~~0742(12)60242-3, 2013.~~
~~Mitchell, J. F. B. and Johns, T. C.: On the modification of global warming by sulphate~~

aerosols. *J. Climate*, 10, 245–267, 1997.

Montgomery, D. R. and Stolar, D. B.: Reconsidering Himalayan river anticlines, *Geomorphology*, 82, 4–15, doi:10.1016/j.geomorph.2005.08.021, 2006.

Moss, R. H., et al.: The next generation of scenarios for climate change research and assessment, *Nature*, 463, 747–756, doi:10.1038/nature08823, 2010.

Nuimura, T., Fujita, K., Yamaguchi, S., and Sharma, R. R.: Elevation changes of glaciers revealed by multitemporal digital elevation models calibrated by GPS survey in the Khumbu region, Nepal Himalaya, 1992–2008, *J. Glaciol.*, 58, 648–656, doi:10.3189/2012JoG11J061, 2012.

Pal, I. and Al-Tabbaa, A.: Long term changes and variability of monthly extreme temperatures in India, *Theor. Appl. Climatol.*, 100, 45–56, doi:10.1007/s00704-009-0167-0, 2010.

Palazzi, E., von Hardenberg, J., and Provenzale, A.: Precipitation in the Hindu Kush Karakoram Himalaya: Observations and future scenarios, *J. Geophys. Res.*, 118, 85–100, doi: 10.1029/2012JD018697, 2013.

Pepin, N. C. and Lundquist, J. D.: Temperature trends at high elevations: patterns across the globe, *Geophys. Res. Lett.*, 35, doi:10.1029/2008GL034026, 2008.

Peters, J., Boleh, T., Buchroithner, M. F., and Bäßler, M.: Glacier Surface Velocities in the Mount Everest Area/Nepal using ASTER and Ikonos imagery, *Proceeding of 10th International Symposium on High Mountain Remote Sensing Cartography*, Kathmandu, Nepal, 313–320, 2010.

Putero, D., T. C., Landi, P., Cristofanelli, A., Marinoni, P., Laj, R., Duchi, F., Calzolari, G. P., Verza and P. Bonasoni, Influence of open vegetation fires on black carbon and ozone variability in the southern Himalayas (NCO-P, 5079 m a.s.l.), *Environ. Pollut.*, 184, 597–604, doi: 10.1016/j.envpol.2013.09.035, 2013.

Qian, Y., Flanner, M., Leung, L., and Wang, W.: Sensitivity studies on the impacts of Tibetan plateau snowpack pollution on the Asian hydrological cycle and monsoon climate, *Atmos. Chem. Phys.*, 11, 1929–1948, doi:10.5194/acp-11-1929-2011, 2011.

Quincey, D. J., Luckman, A., and Benn, D.: Quantification of Everest region glacier velocities between 1992 and 2002, using satellite radar interferometry and feature tracking, *J. Glaciol.*, 55, 596–606, doi: 10.3189/002214309789470987, 2009.

Ramanathan, V., Chung, C., Kim, D., Bettge, T., Buja, L., Kiehl, J. T., Washington, W. M., Fu, Q., Sikka, D. R., and Wild, M.: Atmospheric brown clouds: Impacts on South Asian climate and hydrological cycle. *Proc. Natl. Acad. Sci. U.S.A.*, 102, 5326–5333, doi: 10.1073/pnas.0500656102, 2005.

Ramanathan, V., Li, F., Ramana, M. V., Praveen, P. S., Kim, D., Corrigan, C. E., Nguyen, H., Stone, E. A., Schauer, J. J., Carmichael, G. R., Adhikary, B., and Yoon, S. C.: Atmospheric brown clouds: Hemispherical and regional variations in long-range transport, absorption, and radiative forcing, *J. Geophys. Res.*, 112, D22, doi:10.1029/2006JD008124, 2007.

Rangwala, I. and Miller, J. R.: Climate change in mountains: a review of elevation-dependent warming and its possible causes, *Climatic Change*, 114, 527–547,

doi:10.1007/s10584-012-0419-3, 2012.

Rangwala, I., Barsugli, J., Cozzetto, K., Neff, J., and Prairie, J.: Mid 21st century projections in temperature extremes in the southern Colorado Rocky Mountains from regional climate models, *Clim Dyn.*, 39, 1823–1840, doi:10.1007/s00382-011-1282-z, 2012.

Rikiishi, K. and Nakasato, H.: Height dependence of the tendency for reduction in seasonal snow cover in the Himalaya and the Tibetan Plateau region, 1966–2001, *Ann. Glaciol.*, 43, 369–377, doi: http://dx.doi.org/10.3189/172756406781811989, 2006.

Salerno, F., Buraschi, E., Bruccoleri, G., Tartari, G., and Smiraglia, C.: Glacier surface area changes in Sagarmatha National Park, Nepal, in the second half of the 20th century, by comparison of historical maps, *J. Glaciol.*, 54, 738–752, 2008.

Salerno, F., Viviano, G., Mangredi, E. C., Caroli, P., Thakuri, S., and Tartari, G.: Multiple Carrying Capacities from a management oriented perspective to operationalize sustainable tourism in protected area, *J. Environ. Manage.*, 128, 116–125, doi:10.1016/j.jenvman.2013.04.043, 2013.

Salerno, F., Gambelli, S., Viviano, G., Thakuri, S., Guyennon, N., D’Agata, C., Diolaiuti, G., Smiraglia, C., Stefani, F., Bochiola, D., and Tartari, G.: High alpine ponds shift upwards as average temperature increase: A case study of the Ortles-Cevedale mountain group (Southern alps, Italy) over the last 50 years, *Global Planet. Change*, doi: 10.1016/j.gloplacha.2014.06.003, 2014.

Salerno, F., Thakuri, S., D’Agata, C., Smiraglia, C., Manfredi, E. C., Viviano, G., and Tartari, G.: Glacial lake distribution in the Mount Everest region: Uncertainty of measurement and conditions of formation, *Global Planet. Change*, 92–93, 30–39, doi:10.1016/j.gloplacha.2012.04.001, 2012.

Scherler, D., Bookhagen, B., and Strecker, M.R.: Spatially variable response of Himalayan glaciers to climate change affected by debris cover, *Nature Geosci.*, 4, 156–159, doi:10.1038/ngeo1068, 2011.

Schneider, T.: Analysis of incomplete climate data: Estimation of mean values and covariance matrices and imputation of missing values, *J. Clim.*, 14, 853–871, doi:10.1175/1520-0442(2001)014<0853:AOICDE>2.0.CO;2, 2001.

Sellegrì, K., Laj, P., Venzac, H., Boulon, J., Picard, D., Villani, P., Bonasoni, P., Marinoni, A., Cristofanelli, P., and Vuillermoz, E.: Seasonal variations of aerosol size distributions based on long-term measurements at the high-altitude Himalayan site of Nepal Climate Observatory Pyramid (5079 m), Nepal, *Atmos. Chem. Phys.*, 10, 10679–10690, doi:10.5194/acp-10.10679-2010, 2010.

Sen, P. K.: Estimates of the regression coefficient based on Kendall’s Tau, *J. Am. Assoc.*, 63, 1379–1389, doi:10.2307/2285891, 1968.

Shekhar, M. S., Chand, H., Kumar, S., Srinivasan, K., and Ganju, A.: Climate change studies in the western Himalaya, *Ann. Glaciol.*, 51, 105–112, doi:10.3189/172756410791386508, 2010.

Shrestha, A. B., Wake, C. P., Mayewski, P. A., and Dibb, J. E.: Maximum temperature

~~trends in the Himalaya and its vicinity: An analysis based on temperature records from Nepal for the period 1971–94, J. Clim., 12, 2775–5561, doi:10.1175/1520-0442(1999)012<2775:MTTITH>2.0.CO;2, 1999.~~

~~Singh, P. and Kumar, N.: Effect of orography on precipitation in the western Himalayan region, J. Hydrol., 199, 183–206, doi:10.1016/S0022-1694(96)03222-2, 1997.~~

~~Su, B. D., Jiang, T., and Jin, W. B.: Recent trends in observed temperature and precipitation extremes in the Yangtze River basin, China, Theor. Appl. Climatol., 83, 139–151, doi:10.1007/s00704-005-0139-y, 2006.~~

~~Tartari, G., Vuillermoz, E., Manfredi, E. C., and Toffolon, R.: CEOP High Elevations Initiative, GEWEX News, Special Issue, 19(3), 4–5, 2009.~~

~~Tartari, G., Salerno, F., Buraschi, E., Bruccoleri, G., and Smiraglia, C.: Lake surface area variations in the North-Eastern sector of Sagarmatha National Park (Nepal) at the end of the 20th Century by comparison of historical maps, J. Limnol., 67, 139–154, doi:10.4081/jlimnol.2008.139, 2008.~~

~~Tartari, G., Verza, P., and Bertolami, L.: Meteorological data at PYRAMID Observatory Laboratory (Khumbu Valley, Sagarmatha National Park, Nepal), in Limnology of high-altitude lakes in the Mt. Everest Region (Nepal), edited by: Lami, A. and Giussani, G., Mem. Ist. Ital. Idrobiol., 57, 23–40, 2002.~~

~~Thakuri, S., Salerno, F., Smiraglia, C., Bolch, T., D'Agata, C., Viviano, G., and Tartari, G.: Tracing glacier changes since the 1960s on the south slope of Mt. Everest (central southern Himalaya) using optical satellite imagery, The Cryosphere, 8, 1297–1315, doi:10.5194/tc-8-1297-2014, 2014.~~

~~Thiemeßl, M. J., Gobiet, A., and Heinrich, G.: Empirical-statistical downscaling and error correction of regional climate models and its impact on the climate change signal, Climatic Change, 112, 449–468, doi:10.1007/s10584-011-011-0224-4, 2012.~~

~~Turner, A. G. and Annamalai, H.: Climate change and the South Asian summer monsoon, Nat. Clim. Change, 2, 587–595, doi:10.1038/nclimate1495, 2012.~~

~~Ueno K. and Aryal, R.: Impact of tropical convective activity on monthly temperature variability during non-monsoon season in the Nepal Himalayas, J. Geophys. Res., 113, D18112, doi:10.1029/2007JD009524, 2008.~~

~~UNEP (United Nations Environment Programme)/WCMC (World Conservation Monitoring Centre): Sagarmatha National Park, Nepal, in Encyclopedia of Earth, edited by: McGinley, M. and Cleveland, C. J., Environmental Information Coalition, National Council for Science and the Environment, Washington, DC, 2008.~~

~~Venzac, H., Sellegri, K., Laj, P., Villani, P., Bonasoni, P., Marinoni, A., Cristofanelli, P., Calzolari, F., Fuzzi, S., Decesari, S., Facchini, M. C., Vuillermoz, E., and Verza, G. P.: High-frequency new particle formation in the Himalayas, Proc. Natl. Acad. Sci. USA, 105, 15666–15671, doi:10.1073/pnas.0801355105, 2008.~~

~~Vuille, M.: Climate variability and high-altitude temperature and precipitation, in Encyclopedia of snow, ice and glaciers, edited by: Singh, V. P. et al., Springer, pp. 153–156, 2011.~~

~~Wagnon, P., Vincent, C., Arnaud, Y., Berthier, E., Vuillermoz, E., Gruber, S., Ménégoz,~~

~~M., Gilbert, A., Dumont, M., Shea, J. M., Stumm, D., and Pokhrel, B. P.: Seasonal and annual mass balances of Mera and Pokalde glaciers (Nepal Himalaya) since 2007, *The Cryosphere*, 7, 1769–1786, doi:10.5194/tc-7-1769-2013, 2013.~~

~~Washington, W. M. and Parkinson, C. L.: An introduction to three-Dimensional Climate Modeling, 2nd Edition, University Science Books, Sausalito, 2005.~~

~~Wu, B.: Weakening of Indian summer monsoon in recent decades, *Adv. Atmos. Sci.* 22(1), 21–29, doi:10.1007/BF02930866, 2005.~~

~~Yang J., Tan, C., and Zhang, T.: Spatial and temporal variations in air temperature and precipitation in the Chinese Himalayas during the 1971–2007, *Int. J. Climatol.*, 33, 2622–2632, doi:10.1002/joc.3609, 2012.~~

~~Yang, X., Zhang, Y., Zhang, W., Yan, Y., Wang, Z., Ding, M., and Chu, D.: Climate change in Mt. Qomolangma region since 1971, *J. Geogr. Sci.*, 16, 326–336, doi:10.1007/s11442-006-0308-7, 2006.~~

~~Yao, T., Thompson, L., Yang, W., Yu, W., Gao, Y., Guo, X., Yang, X., Duan, K., Zhao, H., Xu, B., Pu, J., Lu, A., Xiang, Y., Kattel, D. B., and Joswiak, D.: Different glacier status with atmospheric circulations in Tibetan Plateau and surroundings, *Nat. Clim. Change*, 2, 663–667, doi:10.1038/nclimate1580, 2012.~~

~~You, Q., Kang, S., Pepin, N., Flügel, W., Yan, Y., Behrawan, H., and Huang, J.: Relationship between temperature trend magnitude, elevation and mean temperature in the Tibetan Plateau from homogenized surface stations and reanalysis data, *Global Planet. Change*, 71, 124–133, doi:10.1016/j.gloplacha.2010.01.020, 2010.~~

~~Zhao, H., Xu, B., Yao, T., Wu, G., Lin, S., Gao, J., and Wang, M.: Deuterium excess record in a southern Tibetan ice core and its potential climatic implications, *Clim. Dyn.*, 38, 1791–1803, doi:10.1007/s00382-011-1161-7, 2012.~~

1403 *Table 1. List of surface stations belonging to PYRAMID Observatory Laboratory*
1404 *network located along the south slopes of Mt. Everest (upper DK Basin).*

Station ID	Location	Latitude °N	Longitude °E	Elevation m a.s.l.	Sampling Frequency	Data Availability		% of daily missing data	
						From	To	Air Temperature	Precipitation
AWS3	Lukla	27.70	86.72	2660	1 hour	02/11/2004	31/12/2012	23	20
AWSN	Namche	27.80	86.71	3570	1 hour	27/10/2001	31/12/2012	21	27
AWS2	Pheriche	27.90	86.82	4260	1 hour	25/10/2001	31/12/2013	15	22
AWS0	Pyramid	27.96	86.81	5035	2 hours	01/01/1994	31/12/2005	19	16
AWS1	Pyramid	27.96	86.81	5035	1 hour	01/01/2000	31/12/2013	10	21
ABC	Pyramid	27.96	86.82	5079	1 hour	01/03/2006	31/12/2011	5	1
AWS4	Kala Patthar	27.99	86.83	5600	10 minutes	01/01/2009	31/12/2013	28	38
AWS5	South Col	27.96	86.93	7986	10 minutes	01/05/2008	31/10/2011	39	100

Table 2. List of ground weather stations located in the Koshi Basin and descriptive statistics of the Sen's slopes for minimum, maximum, and mean air temperatures and total precipitation for the 1994-2012 period. The annual mean air temperature, the total annual mean precipitation, and the percentage of missing daily values is also reported. Level of significance ($^{\circ}$ p -value = 0.1, * p -value = 0.05, ** p -value = 0.01, and *** p -value = 0.001).

ID	Station Name	Latitude	Longitude	Elevation	Air Temperature					Precipitation		
					Annual mean	Missing values	MinT trend	MaxT Trend	MeanT trend	Annual total	Missing values	Prec trend
		$^{\circ}$ N	$^{\circ}$ N	m a.s.l.	$^{\circ}$ C	%	$^{\circ}$ C a^{-1}	$^{\circ}$ C a^{-1}	$^{\circ}$ C a^{-1}	mm	%	mm a^{-1}
KO-S (NEPAL)	1024 DHULIKHEL	27.61	85.55	1552	17.1	2	-0.012	0.041	0.026	1191	10	-25.0 *
	1036 PANCHKHAL	27.68	85.63	865	21.4	10	0.038	0.051 *	0.038 $^{\circ}$	3669	10	-21.9
	1058 TARKE GHYANG	28.00	85.55	2480						1369	3	-1.4
	1101 NAGDAHA	27.68	86.10	850						2484	4	6.6
	1103 JIRI	27.63	86.23	2003	14.4	1	0.013	0.020	0.014 $^{\circ}$	2148	2	1.3
	1202 CHAURIKHARK	27.70	86.71	2619						1786	3	-5.1
	1206 OKHALDHUNGA	27.31	86.50	1720	17.6	2	-0.017	0.042	0.000	1017	2	-23.4 $^{\circ}$
	1210 KURULE GHAT	27.13	86.41	497						1324	4	15.9
	1211 KHOTANG BAZAR	27.03	86.83	1295						1402	6	10.4
	1222 DIKTEL	27.21	86.80	1623						4537	6	-54.3 **
	1301 NUM	27.55	87.28	1497						1469	0	-1.1
	1303 CHAINPUR (EAST)	27.28	87.33	1329	19.1	0	-0.127 *	0.024	-0.064 $^{\circ}$	1540	4	-3.7
	1304 PAKHRIBAS	27.05	87.28	1680	16.7	0	-0.005	0.036 *	0.015	942	6	-9.2 $^{\circ}$
	1307 DHANKUTA	26.98	87.35	1210	20.0	0	-0.002	0.153 ***	0.071 ***	1052	6	-13.1 $^{\circ}$
	1314 TERHATHUM	27.13	87.55	1633	18.2	10	0.033	0.066 $^{\circ}$	0.049 *	2531	5	-41.9 *
	1317 CHEPUWA	27.46	87.25	2590						1429	6	-22.9 $^{\circ}$
	1322 MACHUWAGHAT	26.96	87.16	158						2347	1	2.6
	1403 LUNGTHUNG	27.55	87.78	1780						1966	3	-11.6
	1405 TAPLEJUNG	27.35	87.66	1732	16.6	1	0.060 *	0.085 **	0.071 **	1287	2	-13.6 *
	1419 PHIDIM	27.15	87.75	1205	21.2	7	0.047 *	0.082 **	0.067 **			
	MEAN	27.33	87.00	1587	17.9	2	0.003	0.060 $^{\circ}$	0.029 $^{\circ}$	1527	4	-11.1
	PYRAMID	27.96	86.81	5035	-2.4	0	0.072 ***	0.009	0.044 *	449	0	-13.7 ***
KO-N (TIBET)	DINGRI	28.63	87.08	4,302	3.5	0	0.037 $^{\circ}$	0.041 $^{\circ}$	0.037 *	309	0	-0.1
	NYALAM	28.18	85.97	3,811	4.1	0	0.032 $^{\circ}$	0.036 $^{\circ}$	0.036 $^{\circ}$	616	0	-0.2
	MEAN	28.41	86.53	4,057	3.8	0.1	0.034 $^{\circ}$	0.039 *	0.037 *	463	0	-0.1

Table 3. Descriptive statistics of the Sen's slopes on a seasonal basis for minimum, maximum, and mean air temperatures and total precipitation of weather stations located in the Koshi Basin for the 1994-2012 period. The Nepali and Tibetan stations are aggregated as mean values. Level of significance ($^{\circ}$ p -value = 0.1, * p -value = 0.05, ** p -value = 0.01, and *** p -value = 0.001). Annual and seasonal temperature trends are expressed as $^{\circ}\text{C } \alpha^{-1}\text{y}^{-1}$. Annual precipitation trend is expressed as $\text{mm } \alpha^{-1}\text{y}^{-1}$, while the seasonal precipitation trends are in $\text{mm (4 months) } \alpha^{-1}\text{y}^{-1}$.

Location	Minimum Temperature				Maximum Temperature				Mean Temperature				Total Precipitation			
	Pre-	Monsoon	Post-	Annual	Pre-	Monsoon	Post-	Annual	Pre-	Monsoon	Post-	Annual	Pre-	Monsoon	Post-	Annual
SOUTHERN KOSHI BASIN (KO-S, NEPAL)	0.012	-0.005	-0.001	0.003	0.076 *	0.052	0.069 *	0.060 *	0.043	0.020	0.030	0.030 *	0.8	-8.6	-2.5	-11.1
PYRAMID (NEPAL)	0.067 *	0.041 *	0.151 ***	0.072 ***	0.024	-0.028	0.049	0.009	0.035	0.015	0.124 **	0.044 **	-2.5 **	-9.3 **	-1.4 **	-13.7 ***
NORTHERN KOSHI BASIN (KO-N, TIBET)	0.042 *	0.019	0.086 *	0.034 *	0.023	0.030	0.071 *	0.039 *	0.042 *	0.013	0.084 *	0.037 *	2.2	0.4	-3.3 *	-0.1

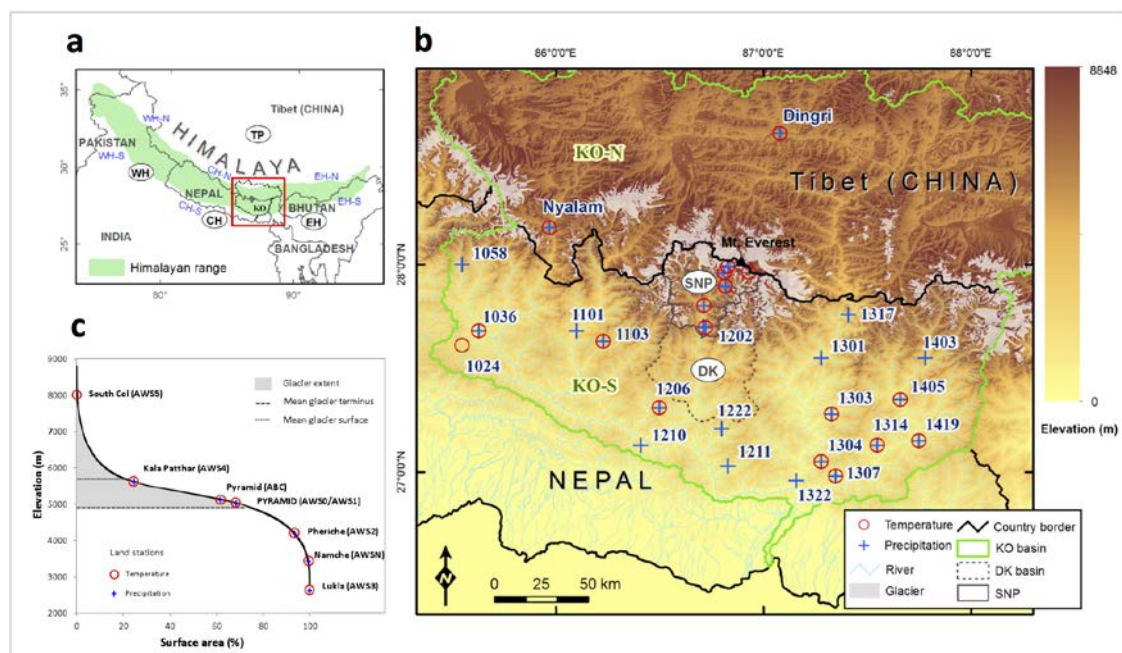


Figure 1. a) Location of the study area in the Himalaya, where the abbreviations WH, CH, EH represents the Western, Central and Eastern Himalaya, respectively (the suffixes -N and -S indicate the northern and southern slopes). b) Focused map on the spatial distribution of all meteorological stations used in this study, where KO and DK stand for the Koshi and Dudh Koshi Basins, respectively; SNP represents the Sagarmatha National Park. c) Hypsometric curve of SNP (upper DK Basin) and altitudinal glacier distribution. Along this curve, the locations of meteorological stations belonging to PYRAMID Observatory Laboratory are presented.

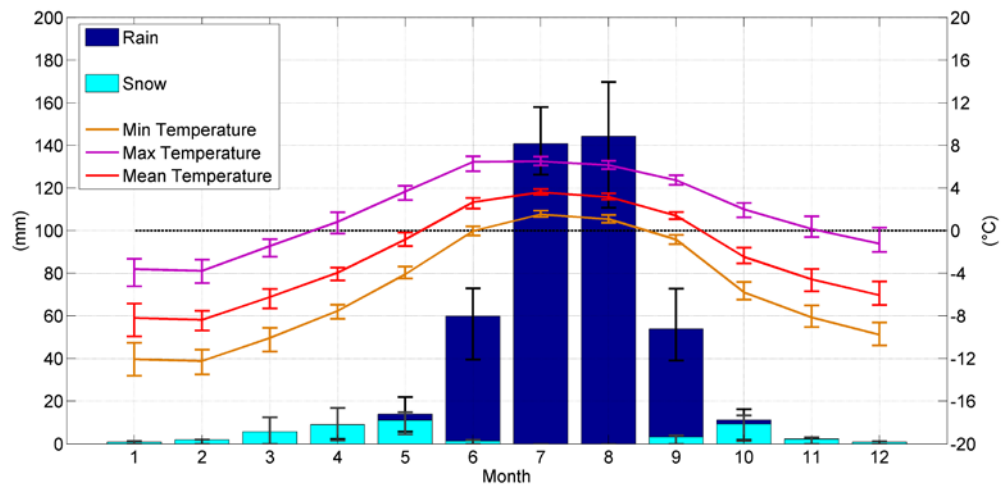


Figure 2. Mean monthly cumulated precipitation subdivided into snowfall and rainfall and minimum, maximum, and mean temperature at 5050 m a.s.l. (reference period 1994-2013). The bars represent the standard deviation.

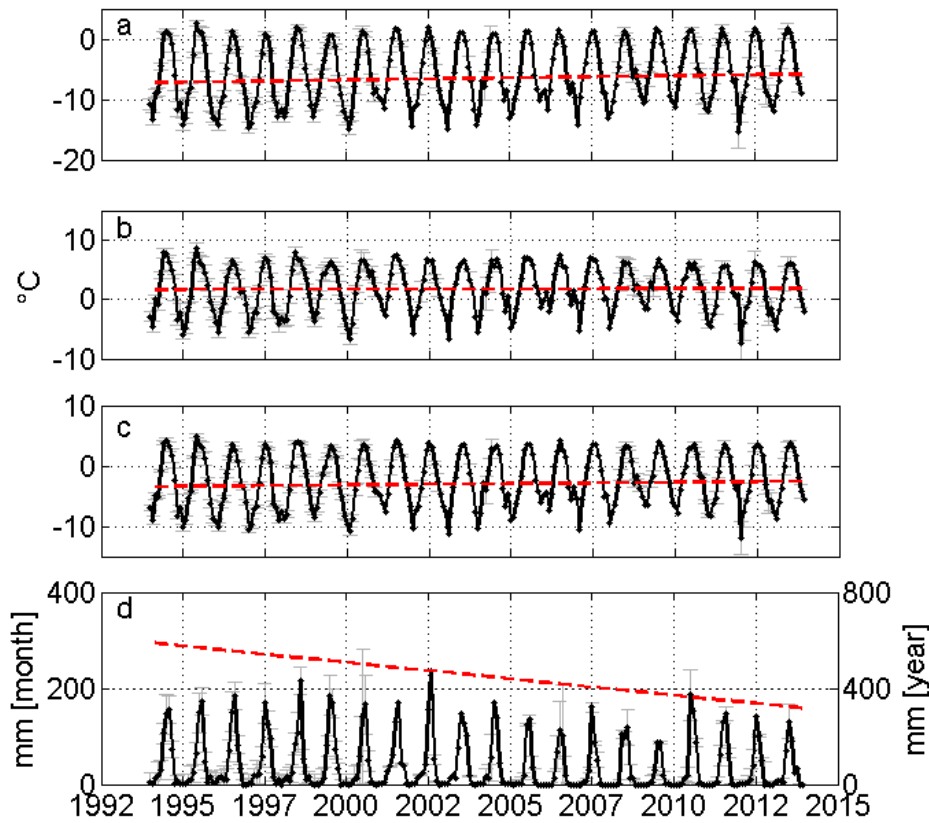


Figure 3. Temperature and precipitation monthly time series (1994-2013) reconstructed at high elevations of Mt. Everest (PYRAMID): minimum (a), maximum (b), and mean temperature (c), and precipitation (d). Uncertainty at 95% is presented as gray bar. The red lines represents the robust linear fitting of the time series characterized by the associated Sen's slope. According to Dytham (2011), the intercepts are calculated by taking the slopes back from every observation to the origin. The intercepts used in here represent the median values of the intercepts calculated for every point (Lavagnini et al., 2011). For precipitation the linear fitting refers at the right axis.

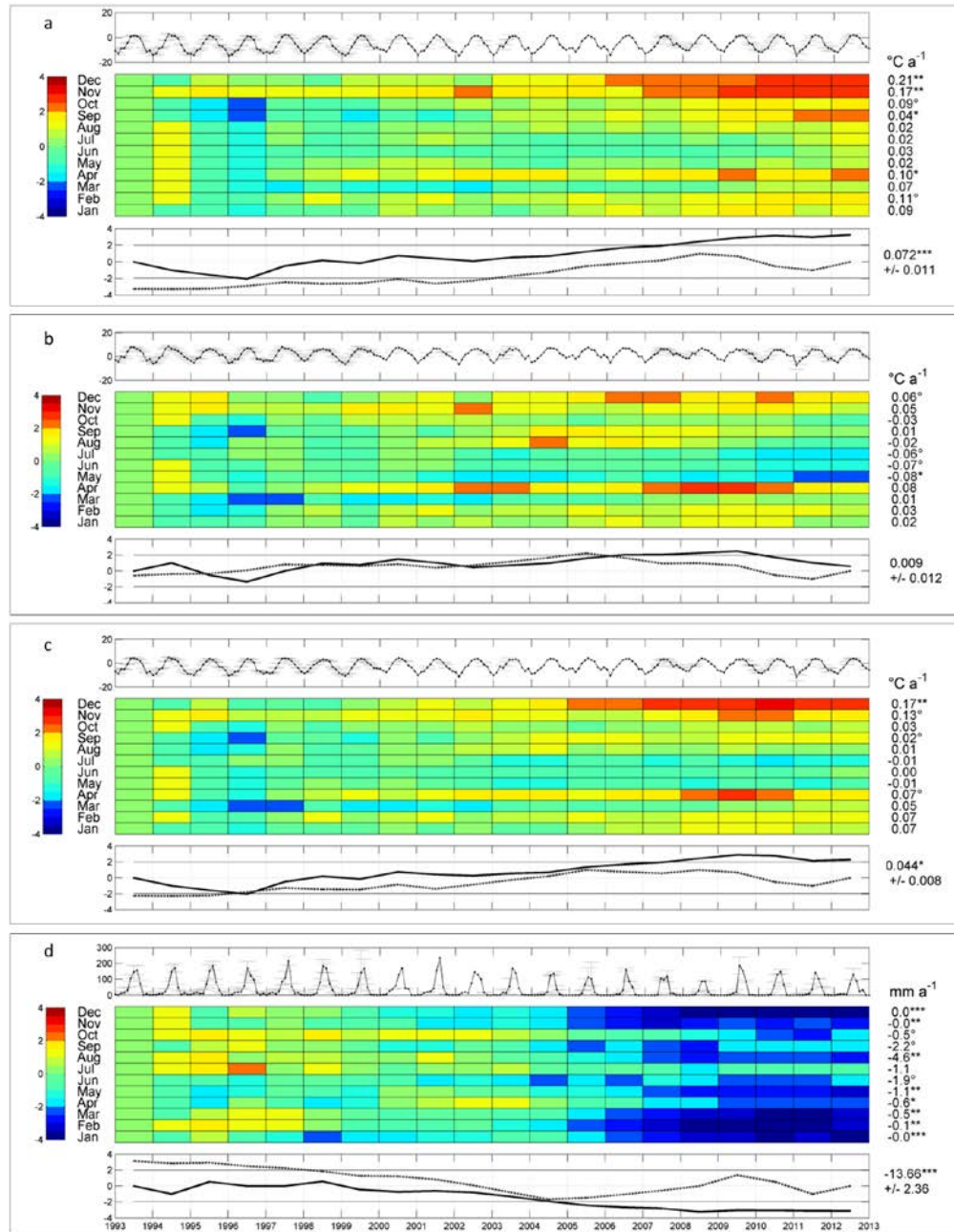


Figure 4. Trend analysis for a) minimum, b) maximum, and c) mean air temperatures and d) total precipitation in the upper DK Basin. The top graph of each meteorological variable shows the monthly trend (dark line) and uncertainty due to the reconstruction process (gray bars). The central grid displays the results of the sequential Mann-Kendall (seqMK) test applied at the monthly level. On the left, the color bar represents the normalized Kendall's tau coefficient $\mu(\tau)$. The color tones below -1.96 and above 1.96 are significant ($\alpha = 5\%$). On the right, the monthly Sen's slopes and the relevant significance levels for the 1994-2013 period ($^{\circ}$ p-value = 0.1, * p-value = 0.05, ** p-value = 0.01, and *** p-value = 0.001). The bottom graph plots the progressive (black line) and retrograde (dotted line) $\mu(\tau)$ applied on the annual scale. On the right, the annual Sen's slope is shown for the 1994-2013 period.

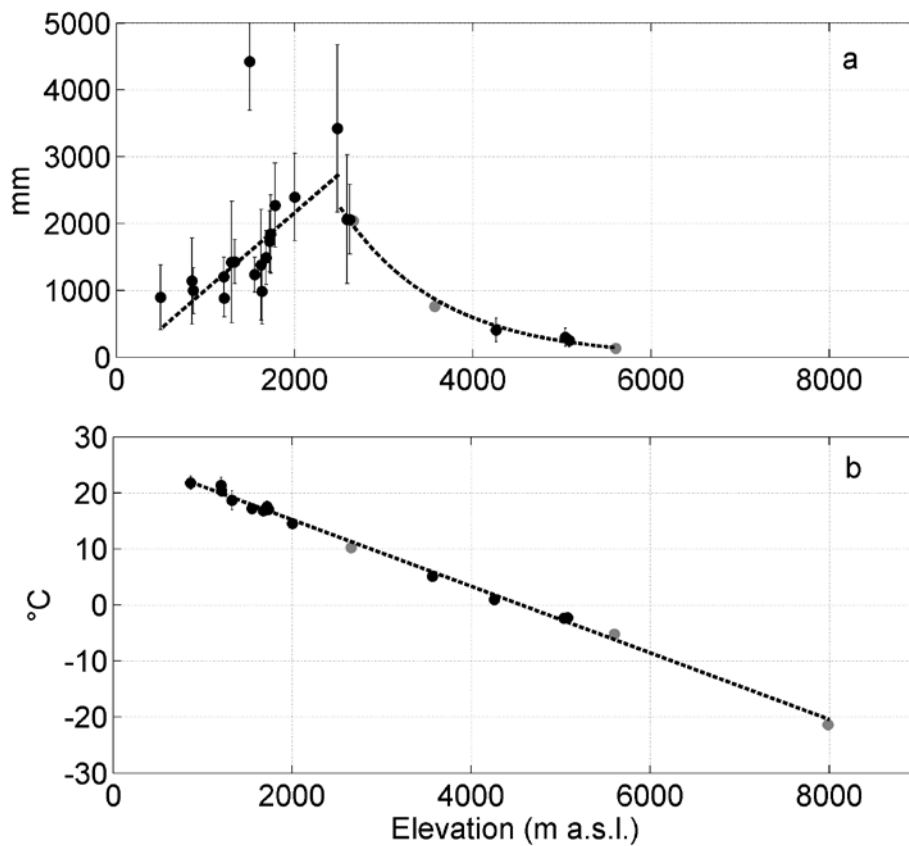


Figure 5. Lapse rates of (a) total annual precipitation in the Koshi Basin for the last 10 years (2003-2012) ~~mean annual air temperature~~ and (b) ~~mean annual air temperature~~ total annual precipitation in the Koshi Basin for the last 10 years (2003-2012). The daily missing data threshold is set to 10%. Only stations presenting at least 5 years of data (black points) are considered to create the regressions (the bars represent two standard deviations). Gray points indicate the stations presenting less than 5 years of data.

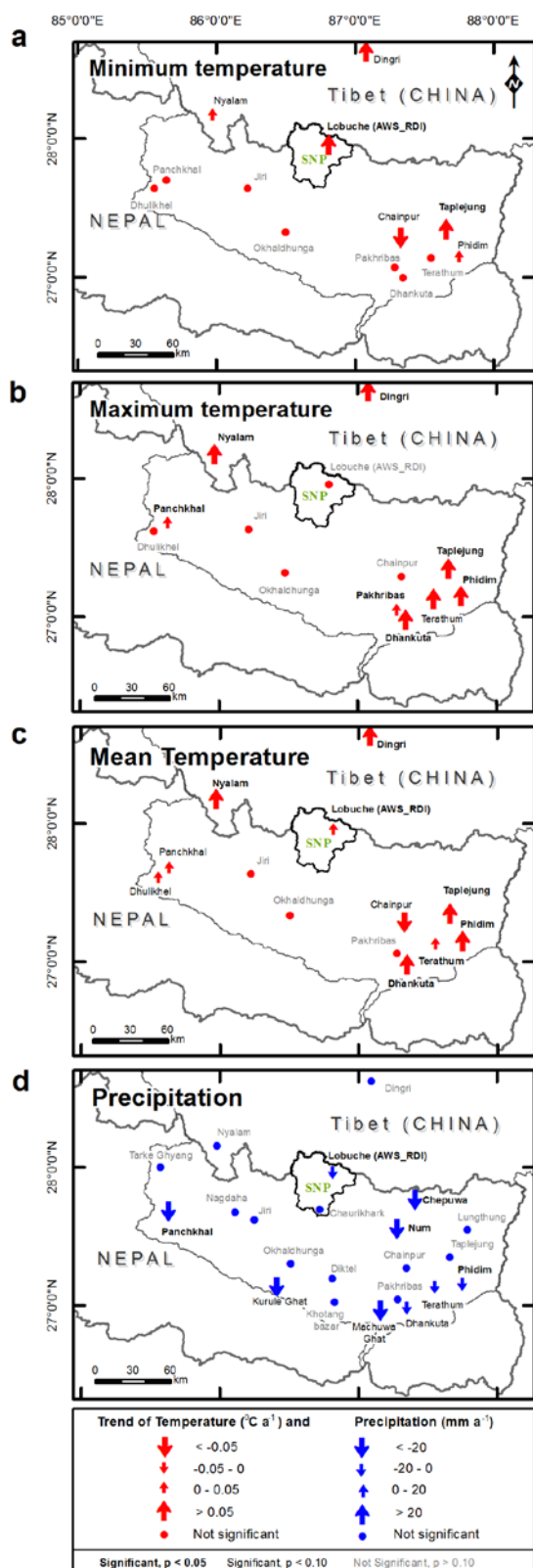


Figure 6. Spatial distribution of the Sen's slopes in the Koshi Basin for minimum (a), maximum (b), and mean (c) air temperature and (d) total precipitation for the 1994-2013 period. Data are reported in Table 2.

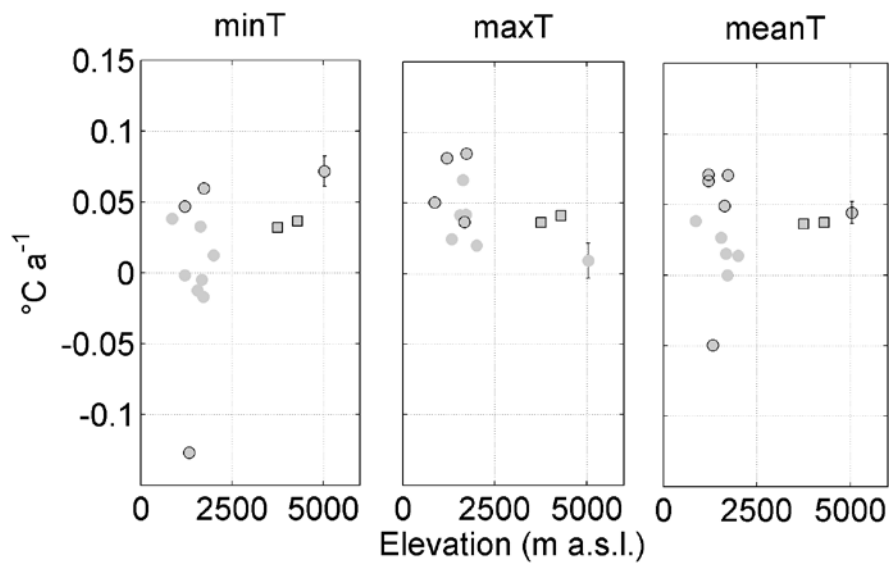


Figure 7. Elevation dependency of minimum (a), maximum (b), and mean (c) air temperatures with the Sen's slopes for the 1994-2013 period. The circle indicates stations with less than 10% of missing daily data, and the star indicates stations showing a trend with $p\text{-value} < 0.1$. The red marker represents the trend and the associated uncertainty (two standard deviations) referred to the reconstructed time series for the AWS1 station (Pyramid). Data are reported in Table 2.

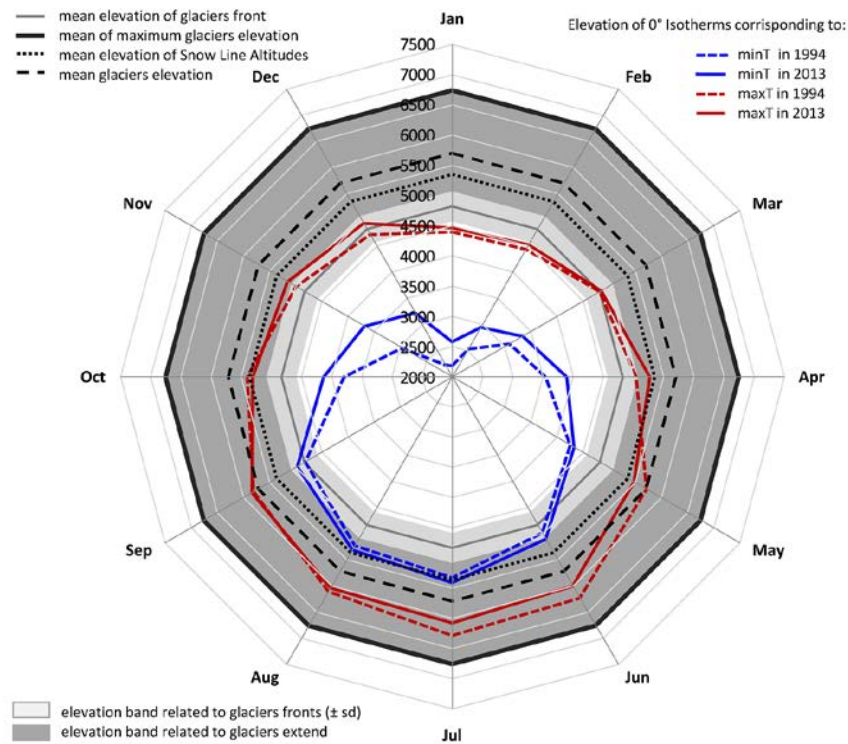
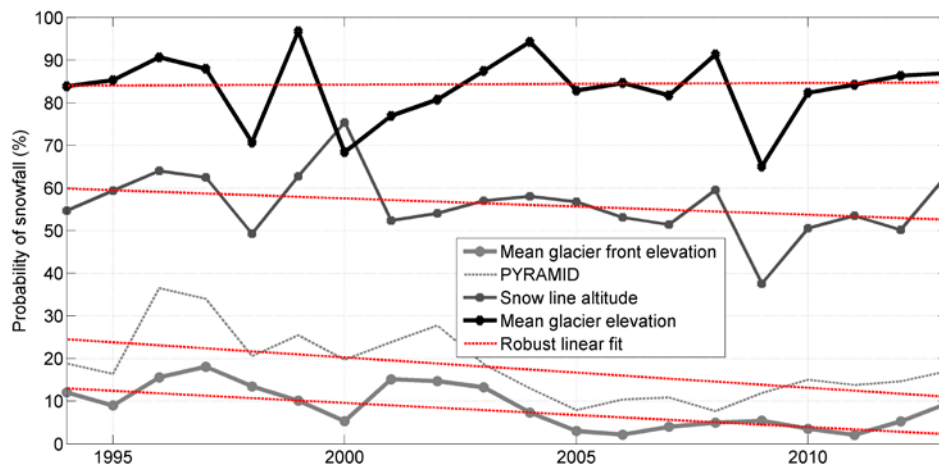


Figure 8. Linkage between the temperature increases and altitudinal glacier distribution. The 0 °C isotherms corresponding to the mean monthly minimum and maximum temperature are plotted for the 1994 and 2013 years according the observed T trends and lapse rates.



1488

1489 *Figure 9. Trend analysis of annual probability of snowfall on total cumulated*
 1490 *precipitation. The red lines represents the robust linear fitting of the time series*
 1491 *characterized by the associated Sen's slope (more details in the caption of Fig. 3).*

Supplementary Material 1

Reconstruction methods of the daily temperature and precipitation time series at Pyramid station (5035 m a.s.l.)

In the following, we describe the missing daily data reconstruction performed on daily T (minimum, maximum, and mean) and Prec time series collected at Pyramid (5035 m a.s.l.) for the 1994-2013 period. As already mentioned in the main text, we consider AWS1 as the reference station (REF) for the reconstruction, which has been operating continuously from 2000 to the present. This station replaced AWS0 (1994-2005). These two stations have a recorded percentage of missing daily values of approximately 20% over the last twenty years (Table S1). The other five stations (ABC, AWSKP, AWS2, AWSN and AWS3) taken into account for the reconstruction process will be referred to as secondary stations. Information regarding the sensors used in the reconstruction process are reported in Table S2.

The time series reconstruction process considers four steps:

- 1) Pre-processing of data
- 2) Infilling method
- 3) Multiple imputation technique
- 4) Monthly aggregation of data

Step 1 – Pre-processing of data

Table 1 shows the sampling frequency of stations (ranging from 10 minutes to 2 hours). After an accurate data quality control according to Ikoma et al., 2007, a daily aggregation of the time series (temporal homogenization) is performed. Daily data have been computed only if the 100% of sub-daily data are available; otherwise, it is considered missing. These rules ensure a maximum quality of daily values with a loss of information limited to the first and last day of the failure events.

Step 2 – Infilling method

The selected daily infilling method is based on a quantile mapping regression (e.g. Déqué 2007). This method estimates a rescaling function F between two time series. This function ensures that the daily cumulated density function (cdf) of a secondary station reproduces the daily cdf of the REF over their over their common observation period. Applying the inverse function (F^{-1}) to each secondary station, a new time series is computed for each of them. In the following, these new time series with the systematic bias corrected are indicated as “*” (e.g., AWS0*, ABC*). In our case the bias is mainly due to the altitude gradient, all stations being located along the same valley (Fig. 1b).

A new time series (REF_filled) has been created merging REF and the * time series according to a priority criterion based on the degree of correlation among data (Fig. S1). The specific rules of computing are described below:

- all available data of REF are maintained in the final reconstruction without any further processing;

- the priority criterion for infilling is based on the magnitude of correlation coefficient (r) between REF and each secondary station, for each variable (Table S1); In case the daily data of the secondary station with higher r is missing the station with the slight lower r is selected.

We can observe from Table S1 that AWS0, located few tens of meters far from REF, presenting $r = 0.99$ and $r = 0.97$ for temperature and precipitation, respectively, has been the first choice. The 82% of missing daily values of temperature and 72% of precipitation are filled using the AWS0*. The second choice is ABC. Together these two stations cover more than the 90% of missing values; the whole infilling procedure allows for filling the 86% and the 91% of the overall missing values of temperature and precipitation, respectively.

Table S1. Correlation coefficients (r) between the reference station (REF) and the other secondary stations for temperature and precipitation. Furthermore the table reports the number of daily data (n) that each station has provided to the reconstruction of the time series.

Stations	Temperature		Precipitation	
	r	n	r	n
AWS0	0.99	2,144 (82.2%)	0.97	2,298 (72.2%)
ABC	0.98	254 (9.7%)	0.84	646 (20.3%)
AWSKP	0.96	48 (1.8%)	0.62	13 (0.4%)
AWS2	0.94	95 (3.6%)	0.81	145 (4.6%)
AWSN	0.92	66 (2.5%)	0.56	78 (2.5%)
AWS3	0.87	0 (0.0%)	0.53	3 (0.1%)
Total infilled values		2,607		3,183

Table S2. List of sensors with measurement height, manufacturer and accuracy. Communicated non-regular intervention as sensors or data logger replacements are reported at the table bottom.

<u>Parameter</u>	<u>Sensor</u>	<u>Manufacturer</u>	<u>Accuracy</u>
<u>AWS0⁽¹⁾</u>			
<u>Air temperature</u>	<u>Precision Linear Thermistor (2m)</u>	<u>MTX</u>	<u>0.1°C</u>
<u>Precipitation</u>	<u>Tipping Bucket (1.5m)</u>	<u>MTX</u>	<u>0.2 mm</u>
<u>Relative humidity</u>	<u>Solid state hygrometer (2m)</u>	<u>MTX</u>	<u>3%</u>
<u>Atmospheric pressure</u>	<u>Aneroid capsule (2m)</u>	<u>MTX</u>	<u>0.5hPa</u>
<u>AWS1</u>			
<u>Air temperature</u>	<u>Thermoresistance (2m)</u>	<u>Lsi-Lastem</u>	<u>0.1°C</u>
<u>Precipitation</u>	<u>Tipping Bucket (1.5m)</u>	<u>Lsi-Lastem</u>	<u>2%</u>
<u>Relative humidity</u>	<u>Capacitive Plate (2m)</u>	<u>Lsi-Lastem</u>	<u>2.5%</u>
<u>Atmospheric pressure</u>	<u>Slice of Silica (2m)</u>	<u>Lsi-Lastem</u>	<u>1hPa</u>
<u>ABC</u>			
<u>Air temperature</u>	<u>Thermoresistance (2m)</u>	<u>Vaisala</u>	<u>0.3°C</u>
<u>Precipitation</u>	<u>Acoustic (2m)</u>	<u>Vaisala</u>	<u>5%</u>
<u>Relative humidity</u>	<u>Capacitive Plate (2m)</u>	<u>Vaisala</u>	<u>3%-5%</u>
<u>Atmospheric pressure</u>	<u>Slice of Silica (2m)</u>	<u>Vaisala</u>	<u>0.5 hPa</u>
<u>AWSKP</u>			
<u>Air temperature</u>	<u>Thermoresistance (2m)</u>	<u>Lsi-Lastem</u>	<u>0.1°C</u>
<u>Precipitation</u>	<u>Tipping Bucket (1.5m)</u>	<u>Lsi-Lastem</u>	<u>1%</u>
<u>Relative humidity</u>	<u>Capacitive Plate (2m)</u>	<u>Lsi-Lastem</u>	<u>1.5%</u>
<u>Atmospheric pressure</u>	<u>Slice of Silica (2m)</u>	<u>Lsi-Lastem</u>	<u>1hPa</u>
<u>AWS2⁽²⁾</u>			
<u>Air temperature⁽³⁾</u>	<u>Thermoresistance (2m)</u>	<u>Lsi-Lastem /Vaisala</u>	<u>0.1°C/0.3°C</u>
<u>Precipitation</u>	<u>Tipping Bucket (1.5m)</u>	<u>Lsi-Lastem</u>	<u>2%</u>
<u>Relative humidity⁽³⁾</u>	<u>Capacitive Plate (2m)</u>	<u>Lsi-Lastem /Vaisala</u>	<u>1.5%/2.5%</u>
<u>Atmospheric pressure⁽³⁾</u>	<u>Slice of Silica (2m)</u>	<u>Lsi-Lastem /Vaisala</u>	<u>1hPa/0.5 hPa</u>
<u>AWSN⁽⁴⁾</u>			
<u>Air temperature</u>	<u>Thermoresistance (2m)</u>	<u>Lsi-Lastem</u>	<u>0.1°C</u>
<u>Precipitation</u>	<u>Tipping Bucket (1.5m)</u>	<u>Lsi-Lastem</u>	<u>2%</u>
<u>Relative humidity</u>	<u>Capacitive Plate (2m)</u>	<u>Lsi-Lastem</u>	<u>2.50%</u>
<u>Atmospheric pressure</u>	<u>Slice of Silica (2m)</u>	<u>Lsi-Lastem</u>	<u>1hPa</u>
<u>AWS3⁽⁵⁾</u>			
<u>Air temperature⁽⁶⁾</u>	<u>Thermoresistance (2m)</u>	<u>Lsi-Lastem /Vaisala</u>	<u>0.1°C/0.3°C</u>
<u>Precipitation</u>	<u>Tipping Bucket (1.5m)</u>	<u>Lsi-Lastem</u>	<u>2%</u>
<u>Relative humidity⁽⁶⁾</u>	<u>Capacitive Plate (2m)</u>	<u>Lsi-Lastem /Vaisala</u>	<u>1.5%/2.5%</u>
<u>Atmospheric pressure⁽⁶⁾</u>	<u>Slice of Silica (2m)</u>	<u>Lsi-Lastem /Vaisala</u>	<u>1hPa/0.5 hPa</u>

⁽¹⁾ dismissed in 2005

⁽²⁾ data logger replacement on 08/12/2010

⁽³⁾ sensors change on 05/2012 to Vaisala sensors

⁽⁴⁾ data logger replacement on 08/10/2010

⁽⁵⁾ data logger replacement on 06/10/2010

⁽⁶⁾ sensors change on 05/2013 to Vaisala sensors

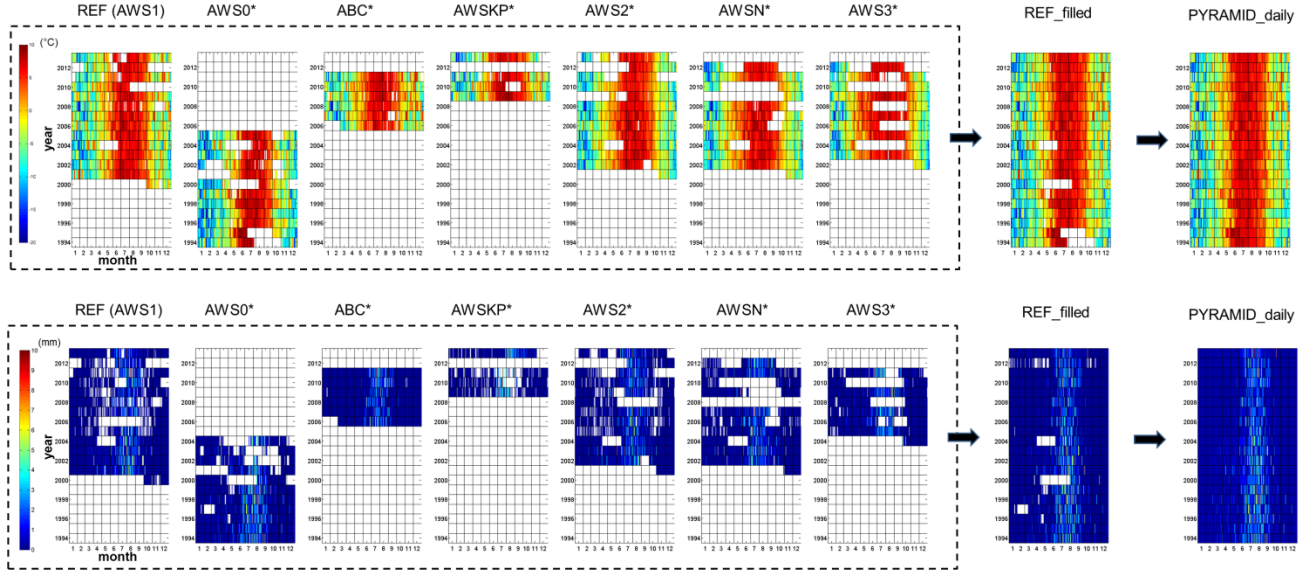


*Figure S1. Scheme followed for the infilling process. Upper panel: daily mean temperature. Lower panel: precipitation. On the left, for each station, the daily data availability and the re-computed values, according to the quantile mapping procedure, are shown. On the right, a new time series (REF_filled) is created by merging REF (reference station) and the * time series, according to a priority criterion described in the text. In case all stations recorded some simultaneous gaps, a multiple imputation technique is applied to obtain the PYRAMID_daily time series.*

The uncertainty associated with REF_filled (σ_{REF_filled}) time series derives from the quantile mapping procedure and in particular from the miss-correlation and possible non stationarity in the quantile relationship.

In order to estimate the σ_{REF_filled} , the probability distribution of the residues between REF and *time series is considered. In order to take into account the possible seasonal variability of the uncertainty, residues have been analyzed on monthly basis.

The Kolmogorov-Smirnov test (Massey, 1951), applied to distribution of the residues, verifies their normality. As a consequence, the daily uncertainty σ_{REF_filled} is estimated as the standard deviation of the residues. The estimated daily uncertainties are reported in Table [S2S3](#).

Table [S2S3](#). Daily uncertainty (expressed as °C and mm for temperature and precipitation, respectively) for each station associated with the daily data infilled through the quantile mapping regression.

Minimum Temperature (minT)												
	Jan	Feb	Mar	Apr	May	Jun	Jul	Aug	Sep	Oct	Nov	Dec
AWS0	0.95	0.98	0.72	0.65	0.49	0.48	0.29	0.35	0.49	0.77	1.09	0.86
ABC	0.82	0.79	1.6	1.29	0.9	0.58	0.66	0.45	0.56	1	0.87	0.89
AWSKP	1.41	1.3	2.25	1.62	1.54	0.84	0.84	0.71	0.65	1.29	1.18	1.61
AWS2	2.06	2.09	2.11	1.85	1.49	1.11	0.88	0.78	0.99	1.99	2.15	1.87
AWSN	2.8	2.44	1.98	1.3	1.14	0.81	0.62	0.72	0.79	1.89	2.95	2.96
AWS3	3.18	2.48	2.35	1.33	1.31	1.25	0.82	0.8	0.88	2.02	3.39	3.23
Maximum Temperature (maxT)												
	Jan	Feb	Mar	Apr	May	Jun	Jul	Aug	Sep	Oct	Nov	Dec
AWS0	0.81	0.9	0.71	1.05	0.65	0.75	0.63	0.61	0.71	1.02	0.74	1.43
ABC	0.61	0.92	1.68	1.2	1.53	1	1.07	0.65	0.75	0.77	0.65	0.62
AWSKP	1.4	1.91	2	1.58	2.12	1.31	1.02	1.07	0.8	1.21	1.49	1.35
AWS2	2.2	2.05	2.07	1.71	1.62	1.13	1.06	0.99	1.12	1.47	1.91	1.9
AWSN	3.41	3.04	2.89	2.25	2.06	1.84	1.42	1.3	1.39	2.14	3.31	3.26
AWS3	4.08	4.11	3.99	2.68	2.6	2.55	2.2	2.23	2.62	3.11	4.15	3.91
Mean Temperature (meanT)												
	Jan	Feb	Mar	Apr	May	Jun	Jul	Aug	Sep	Oct	Nov	Dec
AWS0	0.56	0.7	0.57	0.24	0.28	0.29	0.24	0.24	0.27	0.46	0.45	0.5
ABC	0.34	0.32	1.46	1.02	0.96	0.54	0.72	0.41	0.36	0.59	0.46	0.4
AWSKP	0.91	0.74	2.08	1.3	1.29	0.82	0.58	0.52	0.47	0.94	1.07	1.4
AWS2	1.8	1.88	1.71	1.38	1.1	0.66	0.5	0.43	0.57	1.56	1.88	1.53
AWSN	2.78	2.43	1.85	1.17	1.03	0.69	0.56	0.54	0.64	1.78	2.79	2.83
AWS3	3.09	2.44	2.43	1.41	1.25	1.15	0.75	0.79	1.03	1.91	3.16	3.06
Precipitation (P)												
	Jan	Feb	Mar	Apr	May	Jun	Jul	Aug	Sep	Oct	Nov	Dec
AWS0	0.68	0.22	0.43	0.99	0.61	0.72	1.34	0.93	0.61	0.29	0.38	0.04
ABC	0.02	0.03	0.07	0.28	0.52	1.17	1.91	3.42	1.49	0.1	0.19	0.04
AWSKP	0.27	0.42	0.46	1.04	0.79	1.62	2.79	2.8	1.97	2.09	0.09	0.19
AWS2	0.31	0.15	0.22	0.42	0.7	2.36	4.71	3.68	2.04	1.93	0.6	0
AWSN	0.42	0.66	0.69	1.1	1.19	2.2	5.41	5.13	3.07	1.41	0.27	0.8
AWS3	0.14	0.29	0.43	0.68	0.44	2.06	5.35	5.11	4.57	0.88	0.43	0.11

Step 3 – Multiple imputation technique

Unfortunately, all stations recorded some simultaneous gaps for a given variable: 5.7% and 4.3% for temperature and precipitation, respectively. For these cases, we applied a multiple imputation technique (the Regularized Expectation Maximization algorithm, RegEM; Schneider, 2001) to obtain the final PYRAMID_daily time series (Fig. S1).

This algorithm considers more available meteorological variables. In our case, we feed the procedure with the minimum, maximum and mean temperatures, precipitation, atmospheric pressure and relative humidity. The additional two variables (atmospheric pressure and relative humidity) allowed for a reduction of the estimated uncertainty associated with the computing of these missing data (σ_{RegEM}).

RegEM has been applied to the daily missing data on a monthly basis, considering the possible seasonal effect on the uncertainty. Table S3 reports the number of days imputed to the complete PYRAMID_daily time series for each month and for each variable. The daily standard error σ_{RegEM} estimated by the RegEM algorithm (Table S4S5) has been associated with each imputed data filled into the complete and final time series reconstructions for daily minimum, maximum, and mean temperatures and precipitation.

Table S3S4. Number of days imputed through RegEM

Variable	Jan	Feb	Mar	Apr	May	Jun	Jul	Aug	Sep	Oct	Nov	Dec
minT	0	1	1	35	87	48	68	71	60	33	10	0
maxT	0	1	1	35	87	48	68	71	60	33	10	0
meanT	0	1	1	35	87	48	68	71	60	33	10	0
Prec	13	31	14	52	99	48	31	9	1	9	4	0

Table S4S5. Uncertainty (°C and mm for temperature and precipitation, respectively) associated to the daily imputed thought RegEM

Variable	Jan	Feb	Mar	Apr	May	Jun	Jul	Ago	Sep	Oct	Nov	Dic
minT	-	3.25	2.89	2.34	2.21	1.95	0.83	0.96	1.37	2.54	2.46	-
maxT	-	3.64	3.22	2.82	2.47	1.87	1.34	1.31	1.44	2.30	2.55	-
meanT	-	3.20	2.82	2.34	2.07	1.58	0.72	0.84	1.16	2.17	2.29	-
p	0.18	0.35	0.65	0.86	0.93	2.73	4.54	4.51	2.73	1.59	0.69	-

Step 4- Monthly aggregation

Finally, the PYRAMID_daily time series, for each variable, have been aggregated on the monthly scale (hereinafter referred to as PYRAMID). The uncertainty associated with each value of the PYRAMID (named σ_m) is estimated considering the propagation of the daily uncertainty to the monthly one through the computation of the mean (for temperature) or of the sum (for precipitation).

The propagation of the uncertainty from the daily data d_i to the monthly one is different if we consider the monthly average M_m (as for temperature) or the monthly accumulation M_c (as for precipitation):

$$\sigma_m = \sqrt{\sum_{j=1}^N \left(\frac{\partial M_m}{\partial d_j} \cdot \sigma_{d_j} \right)^2} = \sqrt{\sum_{j=1}^N \left(\frac{\partial \left(\frac{1}{N} \sum_{i=1}^N d_i \right)}{\partial d_j} \cdot \sigma_{d_j} \right)^2} = \sqrt{\frac{1}{N} \sum_{j=1}^N \sigma_{d_j}^2} \quad (1)$$

$$\text{where } M_m = \frac{1}{N} \sum_{i=1}^N d_i$$

and

$$\sigma_m = \sqrt{\sum_{j=1}^N \left(\frac{\partial M_c}{\partial d_j} \cdot \sigma_{d_j} \right)^2} = \sqrt{\sum_{j=1}^N \left(\frac{\partial \sum_{i=1}^N d_i}{\partial d_j} \cdot \sigma_{d_j} \right)^2} = \sqrt{\sum_{j=1}^N \sigma_{d_j}^2} \quad (2)$$

$$\text{where } M_c = \sum_{i=1}^N d_i$$

N is the number of days of a given month and σ_{d_j} the daily uncertainty as :

$$\left\{ \begin{array}{ll} \sigma_{d_j} = 0 & \text{if the data belongs to the REF} \\ \sigma_{d_j} = \sigma_{REF_filled} & \text{if the data is imputed through infilling step} \\ \sigma_{d_j} = \sigma_{RegEM} & \text{if the data is imputed through RegEM} \end{array} \right\}$$

Finally, we estimated the uncertainty associated with the annual Sen's slopes (1994-2013) of each time series through a Monte Carlo uncertainty analysis (e.g., James and Oldenburg 1997):

- For each month value, a random realization of the normal distribution with zero-mean and σ_m standard deviation is computed.
- This uncertainty is added to each monthly estimate coming from eq. (1) or (2), obtaining a time series perturbed by the uncertainty.
- The Sen's slope and associated p-value is computed.
- The process is repeated until the convergence of the mean value of the Sen's slope and the associated standard deviation. In these regards, we observed that approximately 5000 runs are enough to ensure the convergence with a threshold of $10^{-5} \text{ }^\circ\text{C a}^{-1}$ and $10^{-3} \text{ mm a}^{-1}$ for temperature and precipitation, respectively.

Table [S5-S6](#) reports the Sen's slopes for the 1994-2013 period calculated for each reconstructed monthly time series (PYRAMID), associated intervals of confidence (95%), median p-value and the associated [5% and 95%] quantiles.

Table [S5S6](#). Sen's slopes for the 1994-2013 period calculated for each reconstructed monthly time series (PYRAMID), associated intervals of confidence (95%), median p-value and the associated [5% and 95%] quantiles.

Time series	Sen's slope	Interval of confidence (95%)	p-value	quantiles [5% and 95%]
PYRAMID minT	0.072 $^\circ\text{C a}^{-1}$	+/- 0.011	0.0021	[0.0001-0.0212]
PYRAMID maxT	0.009 $^\circ\text{C a}^{-1}$	+/- 0.012	0.7212	[0.2843-0.9741]
PYRAMID meanT	0.044 $^\circ\text{C a}^{-1}$	+/- 0.008	0.035	[0.0053-0.1443]
PYRAMID Prec	-13.66 mm a^{-1}	+/- 2.36	0.0021	[0.0002-0.0252]

REFERENCES

- Ikoma, E., K. Tamagawa, T. Ohta, T. Koike, and M. Kitsuregawa (2007), QUASUR: Web-based quality assurance system for CEOP reference data, *J. Meteorol. Soc. JPN.*, 85A, 461-473.
- Massey, F. J. (1951), The Kolmogorov-Smirnov Test for Goodness of Fit, *J. Am. Stat. Assoc.*, 46(253), 68-78.

Supplementary Material 2

Further analysis on the non-stationarity of the reconstructed daily precipitation time series at Pyramid station

The analysis described in the following aims at assessing whether the decreasing trend of precipitation observed for the daily time series reconstructed at Pyramid (1994-2013) is due to a reduction of duration or to a reduction of intensity.

To this goal we considered two different periods p , say $p1 = 1994-1998$ and $p2 = 2009-2013$, which correspond to the first and last five years of the whole analysis period $p0 = 1994-2013$. For a given week w , the mean weekly-cumulated precipitation RR_w^p is defined as $RR_w^p = (\sum_{y=1}^N RR_{w,y})/N$, where N is the number of years during the period p .

The difference between the mean weekly-cumulated precipitation RR_w^{p1} and RR_w^{p2} may be attributed to a change in the corresponding duration and/or intensity. To separate the relative contributions, we defined two descriptors:

1-The duration of precipitation for a given week w of the year y is described by the number of wet days $W_{w,y}$, where a “wet day” is defined by the threshold $RR > 1$ mm. Then, the mean W_w^p over a given period p of N years is computed as:

$$W_w^p = \frac{1}{N} \sum_{y=1}^N W_{w,y} \quad (1)$$

2- The daily intensity of precipitation for a given week w of the year y is computed as the cumulative precipitation $RR_{w,y}$ divided by the number of wet days $W_{w,y}$. Then, a mean intensity index $SDII_w^p$ over a given period p of N years is computed as:

$$SDII_w^p = \frac{1}{N} \sum_{y=1}^N \frac{RR_{w,y}}{W_{w,y}} \quad (2)$$

An attempt to quantify the contribution to the variation in precipitation arising from variation in duration and/or intensity is to consider one of the two terms stationary over the whole period. This is a rough approximation as the non-stationarity may not be linear. However, an estimation of the relative contribution arising from the change in duration can be expressed considering the intensity of precipitation as stationary over the whole period $p0$ ($SDII_w^{p0}$) and computing the variation of precipitation due only to a variation in duration, i.e. $(W_w^{p2} - W_w^{p1}) * SDII_w^{p0}$. The relative contribution RLD to the total change $(RR_w^{p2} - RR_w^{p1})$ can be estimated as:

$$RLD = \frac{(W_w^{p2} - W_w^{p1}) * SDII_w^{p0}}{(RR_w^{p2} - RR_w^{p1})} * 100 \quad (3)$$

The indexes proposed above are shown in figure S6 in dark blue area for the 1994-1998 period and light blue area for the 2009-2013 period for the W_w^p , $SDII_w^p$ and RR_w^p (panel a, b and c respectively). For each index, we defined as residues the difference between the two periods (red bar plot).

The RLD (shown in red on the right axis of the panel c) indicates that the early and late monsoon are more affected by the reduction in duration than intensity, while it is the opposite during the monsoon.

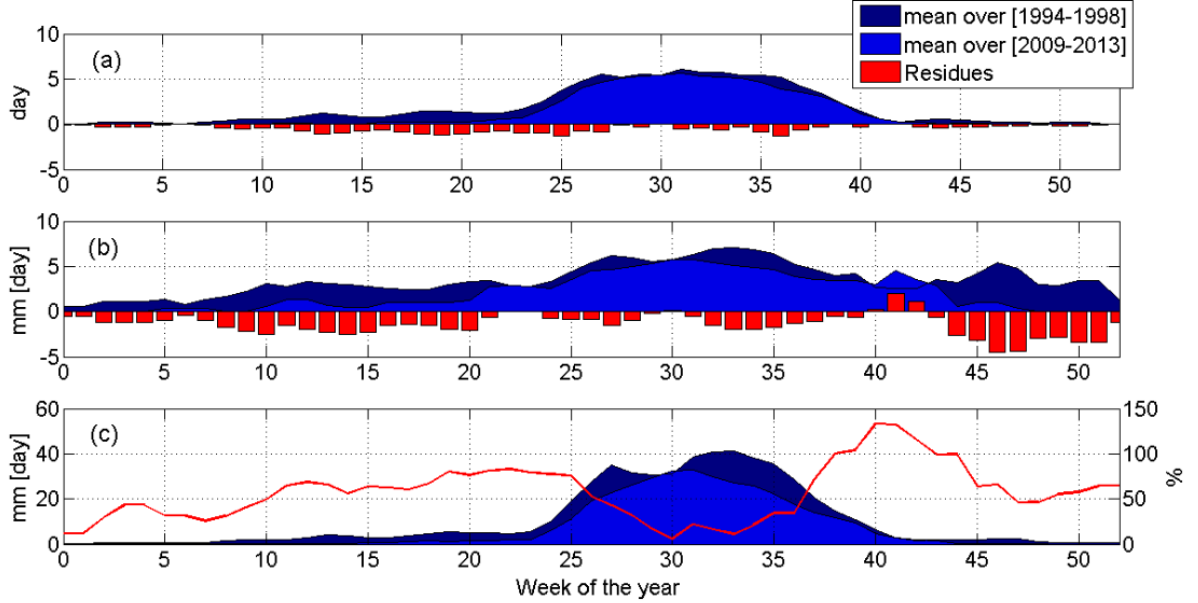


Figure S6. Panel a: Mean number of wet day per week W_w^p . Panel b: Mean daily precipitation intensity $SDII_w^p$ (mm). Panel c: Mean weekly-cumulated precipitation RR_w^p and relative contribution of the change in duration RLD in % (red line)

Supplementary Material 3

Evaluation of the possible underestimation of solid precipitation at Pyramid

The Chaurikhark station (ID 1202) (Fig. 1b, Table 2) is located at 2619 m a.s.l., along the same valley of PYRAMID (Dud Koshi). This station records only daily precipitation with a tipping bucket. Not having the availability of air temperature data, we estimated for this location the mean daily values for the 1994-2013 period through of the lapse rate and the mean daily air temperature series reconstructed in this study at PYRAMID.

The precipitation phase has been taken into account assuming that the probability of snowfall and rainfall depends on the mean daily air temperature (as well as we did for PYRAMID, see the text). In Figure S7 we observe that 86% of precipitation is concentrated during June-September. The probability of snowfall is very low (0.6%) and it is completely concentrated in December, January, and February (the mean temperature of these months is about 5 °C).

We realized the scatter-plot of Figure S8 between their monthly precipitation (averaged on 1994-2013 period) in order to compare the two stations. Data were previously log transformed assuring their normal distribution. First of all, we observe the strong relationship due to the fact that they belong to the same valley, although there are 2400 m of altitudinal range. Secondly, we note the variability between the two stations is higher for those months which record less precipitation (spring and winter). Probably, during these months, PYRAMID underestimates the solid precipitation which fall in liquid form at lower elevation (Chaurikhark). In this regard we realized the graph of Figure S8 for showing the precipitation ratio between PYRAMID and Chaurikhark. We observe that during the monsoon (June-September), period of the year when the probability of snowfall at PYRAMID is very low (4%) (see the text), the precipitation ratio is $21 \pm 3\%$ (standard deviation) that means at 5050 m a.s.l. it rains a fifth respect to 2600 m a.s.l. (see Fig. 5). Outside the monsoon months this ratio decreases to $15 \pm 6\%$. Assuming that this lower ratio if completely attributable to the solid precipitation not captured at high elevations, we calculated an underestimation of $15 \pm 5 \text{ mm y}^{-1}$, corresponding to $3 \pm 1\%$ of the total annual cumulated precipitation at PYRAMID (446 mm y^{-1}).

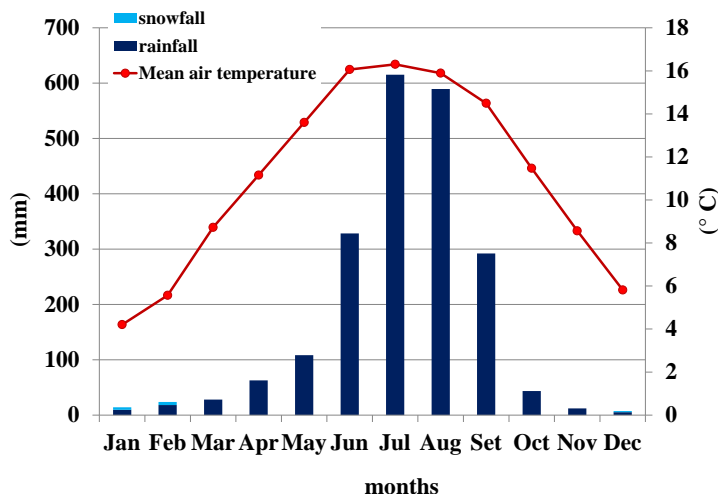


Figure S7. Mean monthly cumulated precipitation subdivided into snowfall and rainfall and mean temperature at Chaurikhark station (ID 1202) (reference period 1994-2013). The bars represent the standard deviation.

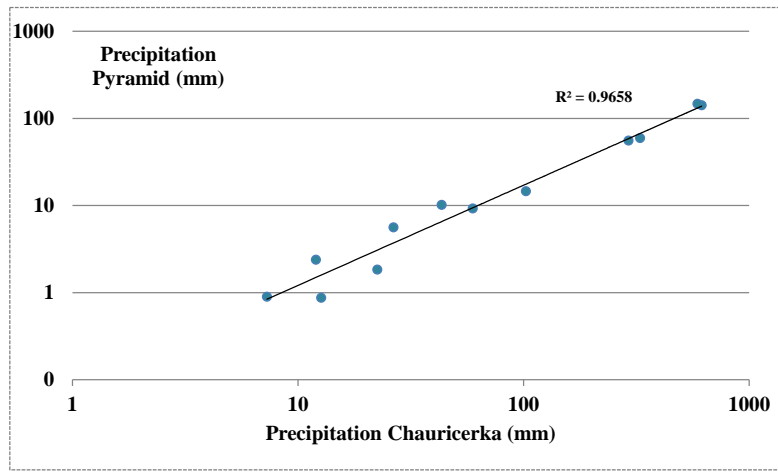


Figure S8. Scatter-plot between the monthly precipitation of PYRAMID and Chaurikhark (averaged on 1994-2013 period).

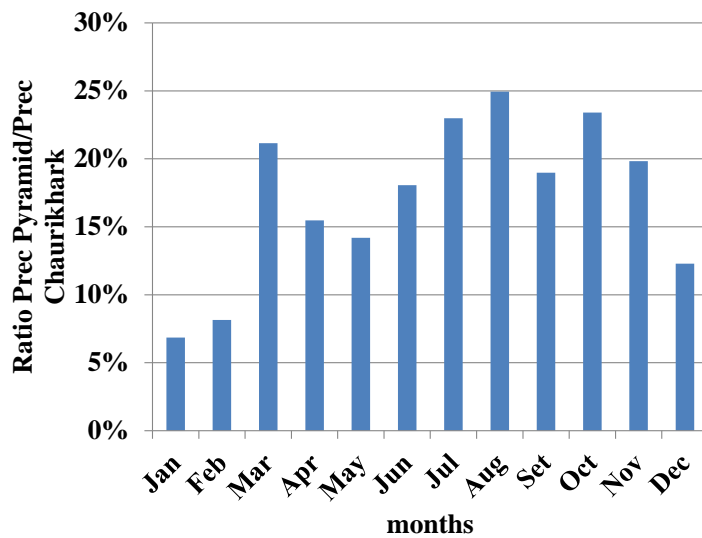


Figure S9. Ratio between the PYRAMID and Chaurikhark total precipitation for each month (averaged on 1994-2013 period).